INVESTIGATION OF ELECTRON IMPACT PROCESSES RELEVANT TO VISIBLE LASERS

M. John W. Boness and H. A. Hyman
Avco Everett Research Laboratory, Inc.
2385 Revere Beach Parkway
Everett MA 02149

Semi–Annual for Period 1 March 1977 to 31 August 1977

Sponsored by
DEFENSE ADVANCED RESEARCH PROJECTS AGENCY
DARPA Order No. 1806

Monitored by
OFFICE OF NAVAL RESEARCH
DEPARTMENT OF THE NAVY
Arlington VA 22217

FOREWORD

Contract No. : N00014-75-C-0064

DARPA Order No. : 1806

Program Code No. : 5E20

Short Title of Work: Lead Atom Transition Forbidden Laser

Principal Investigator: M. John W. Boness, (617) 389-3000, Ext. 451

Scientific Officer: Director, Physics Program,
Physical Sciences Division
Office of Naval Research
800 North Quincy Street
Arlington, Virginia 22217

Effective Date of Contract: 15 August 1974

Contract Expiration Date: 14 November 1977

Amount of Contract: $605, 222

UNCLASSIFIED

SECURITY CLASSIFICATION OF THIS PAGE (When Data Entered)

REPORT DOCUMENTATION PAGE

READ INSTRUCTIONS BEFORE COMPLETING FORM

1. REPORT NUMBER

2. GOVT ACCESSION NO.

3. RECIPIENT'S CATALOG NUMBER

4. TITLE (and Subtitle)

Investigation of Electron Impact Processes Relevant to Visible Lasers

5. TYPE OF REPORT & PERIOD COVERED

Semi-Annual Report
1 Mar 1977 - 31 Aug 1977

6. PERFORMING ORG. REPORT NUMBER

7. AUTHOR(s)

M. John W. Boness and H. A. Hyman

8. CONTRACT OR GRANT NUMBER(s)

N00014-75-C-0064

DARPA Order No. 1806

9. PERFORMING ORGANIZATION NAME AND ADDRESS

Avco Everett Research Laboratory, Inc.
2385 Revere Beach Parkway
Everett, Massachusetts 02149

10. PROGRAM ELEMENT, PROJECT, TASK AREA & WORK UNIT NUMBERS

11. CONTROLLING OFFICE NAME AND ADDRESS

Defense Advanced Research Projects Agency
DARPA Order No. 1806

12. REPORT DATE

31 Aug 77

13. NUMBER OF PAGES

53

14. MONITORING AGENCY NAME & ADDRESS (if different from Controlling Office)

Office of Naval Research
Department of the Navy
Arlington, Virginia 22217

53p.

15. SECURITY CLASS. (of this report)

Unclassified

15a. DECLASSIFICATION/DOWNGRADING SCHEDULE

16. DISTRIBUTION STATEMENT (of this Report)

Approved for public release; distribution unlimited.

17. DISTRIBUTION STATEMENT (of the abstract entered in Block 20, if different from Report)

18. SUPPLEMENTARY NOTES

19. KEY WORDS (Continue on reverse side if necessary and identify by block number)

Cross Sections	Charge Exchange	Excited States
Metastable Atom	Argon	Born Calculations
Electron Spectroscopy	Krypton	Eigenvalues
Fluorescence	Auger Detector	Intermediate Coupling
Glow Discharge	Visible Lasers	Strong Coupling

20. ABSTRACT (Continue on reverse side if necessary and identify by block number)

The emphasis of the work during the reporting period has been placed upon the design and optimization of a glow discharge source of metastable atoms which was subsequently installed in the electron spectrometer system. As a consequence of signal-to-noise problems and long term stability limitations encountered with the energy loss spectroscopy the experiment has been modified and a fluorescence diagnostic substituted for the electrostatic electron energy analyzer. Preliminary experiments involving electron-ground

DD FORM 1 JAN 73 1473 EDITION OF 1 NOV 65 IS OBSOLETE

S/N 0102-014-6601

UNCLASSIFIED

SECURITY CLASSIFICATION OF THIS PAGE (When Data Entered)

state atoms have been performed in order to evaluate the sensitivity of the fluorescence technique. Numerous experimental modifications have been performed in order to reduce the principal source of noise, namely fluorescence emission from the discharge source. Currently experiments are underway to measure the transitions of interest viz.

$$e + Kr^{**}(5sj) \rightarrow e + Kr^{**}(5pj.)$$

by observations of the fluorescence emission

$$Kr^{**}(5pj') \rightarrow Kr^{*}(5sj) + h\nu$$

Born cross sections have been calculated in the intermediate coupling representation for the transition arrays Ar^* (4s; J → 4p; j') and Kr^* (5s; J → 5p; J'). A Unitarized Impace Parameter Born Theory has been employed to estimate the effects of strong coupling effects which are important to low energies. Effective Born cross sections have been computed for a number of transitions of the kind Ar^* (4s → nℓ) and Kr^* (5s → nℓ).

TABLE OF CONTENTS

LIST OF ILLUSTRATIONS

I. INTRODUCTION

Recent advances in the development of high power electric discharge lasers which possess large fractional populations of excited species have emphasized both the lack of, and need for cross section data describing electron collisons with excited species. Modeling calculations[1] indicate that accurate representations of electron-excited state interactions are essential and crucial in attempting to optimize the performance of the laser and the electrical behavior of the discharge.

Until recently data describing electron collisions with excited species was virtually absent from the literature. A growing awareness of the acute need for these data from a practical standpoint has promoted a recent increase in the research activities in this field.[2-6] However, in view of the considerable experimental difficulties in preparing and manipulating beams of excited species data is slow to accumulate and the total amount of available data for collisons of this type is somewhat meager.

The role of the AERL Electron Kinetics program in the DARPA ONR sponsored AERL visible laser program is to relevant electron kinetics data necessary for modeling and optimizing laser performance specifically in

---

1. "KrF Laser Research," AERL 804, April 1976.
2. Long, D. R. and Geballe, R., Phys. Rev. 1, 260 (1970).
3. Lake, M. L. and Garscadden, A., 28th Gaseous Electronics Conference Rolla, Mo. (1975), Paper C-5.
4. Mityurwa, A. A. and Penkin, N. P., Opt. Spectros. 38, 229 (1975).
5. Wilson, W. G. and Williams, W. L., J. Phys. B9, 423 (1976).
6. Tannen, P. D., "Cumulative Ionization and Excitation of Molecular Nitrogen Metastables by Electron Impact," Dissertation (1973), School of Engineering, Air Force Institute of Technology.

the important areas of the KrF scaleup, the excimer laser research program and the area of small-scale discharge studies.

The present AERL Electron Kinetics program was proposed in order to provide absolute cross-section data, particularly with regard to collision processes between electrons and excited atomic and molecular species. The program consists of parallel and complementary experimental and theoretical efforts. Results from these combined program efforts will yield reliable absolute cross-section data covering the range of electron energies encountered in the electric discharges of interest (0.2 to 20 eV).

The rare gas monohalide laser systems which have been the subject of extensive experimental and theoretical investigations at AERL[7, 8, 9] have emerged as extremely promising candidates for satisfying certain goals of the DARPA visible laser program. These studies have identified electron collision processes with metastable states of the rare gas atom constituents as playing a major role in both discharge stability and in determining the equilibrium metastable concentration, which through reaction with the halogen molecule leads to excimer formation.

Therefore the goal of the AERL electron kinetics program is to provide absolute cross sections for electron collisions with the first excited states of the rare gases argon and krypton, both for the metastable substates and for the substates which are optically connected to the ground state.

---

7. Ewing, J.J. and Brau, C.A., Appl. Phys. Lett. 27, 350 (1975).
8. Ewing, J.J. and Brau, C.A., Phys. Rev. A12, 129 (1975).
9. Mangano, J.A. and Jacob, J.H. App. Phys. Lett. 27, 495 (1975).

The approach which has been adopted is to normalize the relative experimental data to the theoretical calculations in the intermediate energy range (above the ionization limit), where stong-coupling effects and resonance phenonema should be minimal, and where the theory should thus be the most accurate. Once the normalization factor is determined, it can be applied to the data over the entire energy range, including very low energies near the excitation threshold where the theory is less reliable. The combined experimental and theoretical effort will therefore be able to provide the absolute cross sections with the level of accuracy needed for laser modeling.

Examples of the transitions of interest are indicated in the partial energy level diagram for krypton shown in Figure 1. In terms of electronic structure the first excited state of krypton resembles the ground state of rubidium. Thus the electron impact excitation cross section for transitions between the first two excited states, 5s → 5p, in krypton should be analogous to the alkali atom resonance transition which is known to be extremely large, of the order 10^{-14} cm^2.

This value is much larger than the various cross sections involving ground state excitation processes. Consequently, once significant fractional populations of the 5s excited state are generated in the discharge then the 5s → 5p excitation process will become the dominant energy loss process for the electrons and attempts to generate higher densities of the 5s state will lead to less efficient operation of the laser, and due to the close proximity of this state to the ionization limit will eventually lead to rapid stepwise ionization and consequent discharge instability.

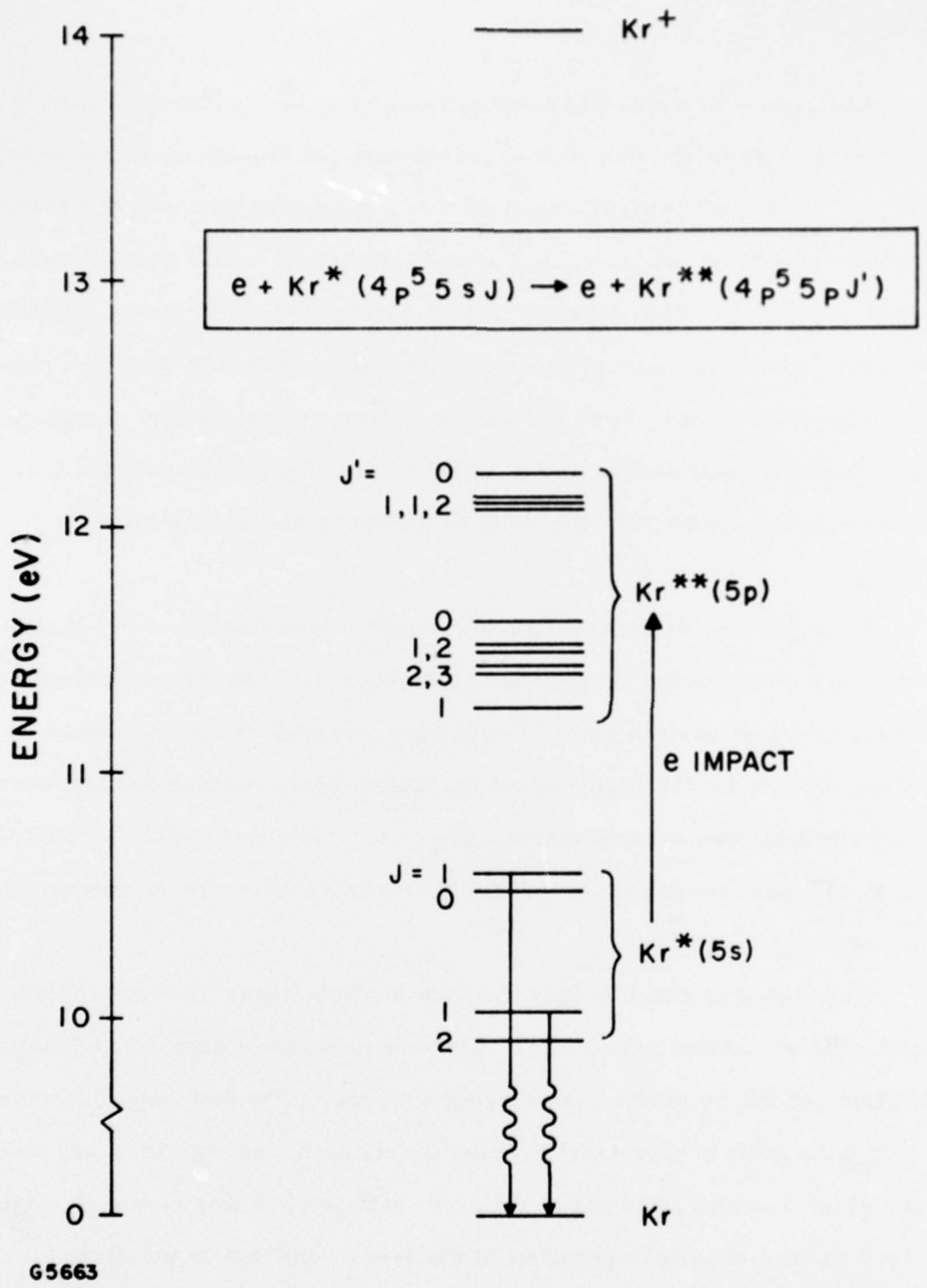

Figure 1 Partial Energy Level Diagram for the Krypton Atom Indicating Electron Excitation Processes of Interest between the 5sj and 5pj' Levels

The experimental apparatus which is described in Section II employs the crossed beams technique and was originally combined with an electron spectrometer to perform electron energy loss analysis and hence provide the required relative excitation cross sections. For reasons which are fully discussed in Section II a fluorescence technique has been substituted for the method of electron energy loss spectroscopy in order to identify and measure the relative excitation functions for the transitions of interest.

The source of metastable atoms employed is a low pressure DC discharge tube. The source has been fully characterized and the design and operation optimized for the production of metastable gas atoms. Using an Auguer metastable atom detector absolute metastable krypton densities in the region of the cross electron and atomic beams have been estimated to be $\sim 10^{7}$ cm^{-3}.

Experiments are currently underway using the fluorescence technique to provide the relative cross sections for excitation from the metastable states for argon and krypton.

The principal results of the theoretical calculations are: (1) the electron impact excitation of metastable argon and krypton is dominated by a single transition (4s → 4p for Ar and 5s → 5p for Kr) with a large cross section $\sim 100\ \pi a_o^2$ at the peak) and (2) strong coupling effects are dominant at low energies for the ns → np transition. In addition, it has been shown that the use of the intermediate coupling representation is required to obtain meaningful results for cross sections between the various substates.

II. EXPERIMENT

During the initial contractual periods an electron gun and electron spectrometer system was designed and fabricated and installed in a doubly differentially pumped bakeable stainless steel vacuum chamber. The associated control circuitry was designed and built and interfaced with the spectrometer system.

During subsequent program periods the performance of the spectrometer system was investigated and various modifications performed as required. In particular since extremely low signals were anticipated in the electron - metastable atom scattering experiment considerable emphasis was placed upon reducing the background noise generated in the system due to strong inelastically scattered electrons.

The emphasis of the work during the present reporting period has been placed upon the design and optimization of a glow discharge source of metastable atoms. This source has been installed in the experimental system and various electron scattering experiments have been attempted. Recognizing that at the present level of metastable densities available from the glow discharge source the electron spectroscopy technique is not capable of providing manageable signal intensities an alternative diagnostic technique was sought. As a consequence the experiment has been modified and a fluorescence diagnostic installed. Preliminary experiments involving electron - ground state atoms have been performed using the technique and currently experiments are underway to measure the transition of interest

viz, $e + Kr^{*}(5sj) \rightarrow e + Kr^{**}(5pj')$

by observing fluorescence from the transition

$$Kr^{**}(5pj') \rightarrow Kr^{*}(5sj) + h\nu$$

A. APPARATUS

The experiment employs the crossed-beam technique, the concept of which is outlined in Figure 2. A low density collimated beam of the atomic or molecular species of interest is collided at right angles with an electron beam of the appropriate energy whose energy spread is small compared with the mean energy. In general, a wide variety of diagnostic techniques can be employed to measure the electron scattering cross sections. The merits of the various methods were discussed at length in the original AERL Electron Kinetics Program Proposal, which concluded that the electron spectroscopy of the inelastically scattered electrons offered the broadest application compared to any other single technique. However, recognizing that on occasion other diagnostics might be preferred or required for certain processes, the apparatus was constructed in such a way as to permit the addition of these refinements without major modification to the system.

Calculations which model electric discharges in gases are insensitive to structure in the various electron excitation cross sections, if it is narrow compared with the width of the electron energy distribution which exists in the plasma. The objective of this program, therefore, is to provide the broad features of the energy dependence of the various excitation cross sections over the energy range of interest, ~ 0.2 to 20 eV. Since it is unnecessary to employ a high resolution electron beam source, a rather

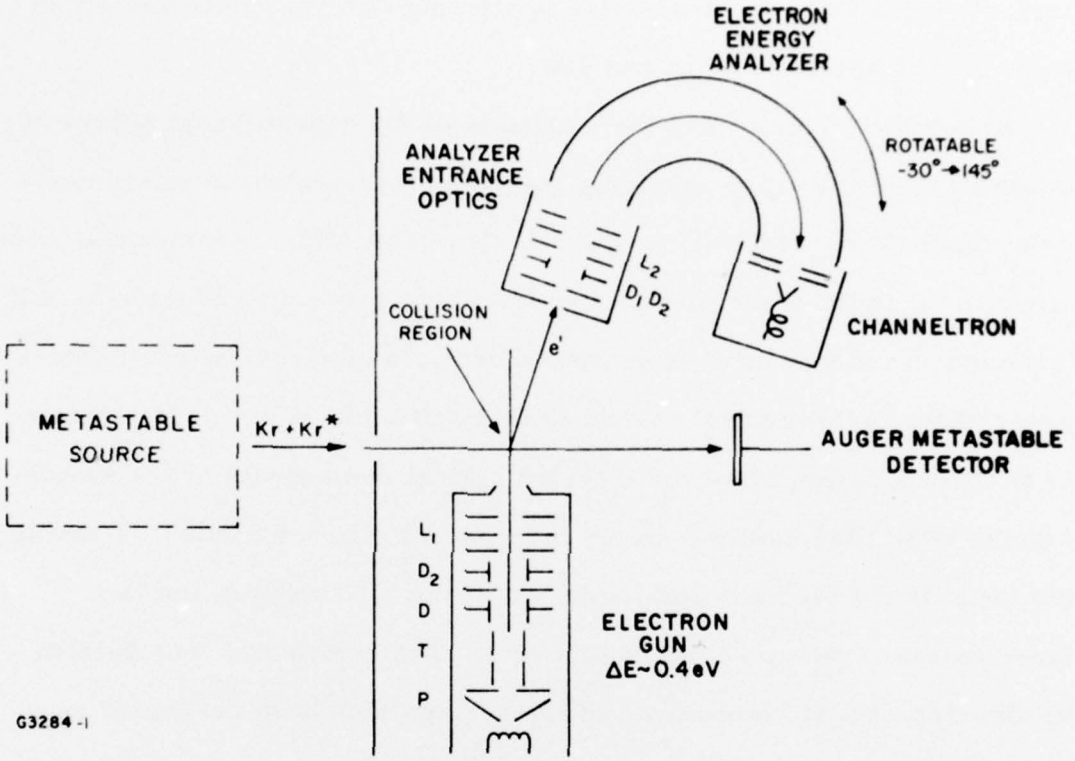

Figure 2 Schematic of the Crossed Beams Apparatus for Electron Scattering from Metastable States of Rare Gases

simple design of electron gun is adopted where the emphasis is placed upon intensity rather than resolution in order to generate reasonable scattered electron currents from the metastable scattering species whose density in the beam is anticipated to be rather low.

As previously explained the emphasis of the experimental aspect of the program is placed upon providing relative cross section measurements over the range from threshold to ~20 eV. It is essential therefore that over this energy range the transmission and focussing properties of the electron spectrometer be independent of energy in order to ensure constant relative accuracy of the measurement. Thus considerable effort has been directed towards careful design of all the electron optical components of the system in order to obtain the desired energy independent characteristics. Central to this issue is the electron optical design of the electron gun and the analyzer entrance optics shown in Figure 2. The design and construction of the electron optical components of the system have been described in detail in a previous semi-annual reports.[10, 11] During the preceding six-monthly period of the program considerable effort was directed towards reducing the background signal arising from strong scattered electrons. This signal was practically eliminated in the angular scattering range $20^{o} \rightarrow 135^{o}$ by the installation of the device shown in Figure 3. The background signal arose from collisons between the primary e-beam and various

---

10. Investigation of Electron Impact Processes Relevant to Visible Lasers. Boness, M. J. and Hyman, H. A. AERL Semi-Annual Report March-Aug. 1976.

11. Investigation of Electron Impact Processes Relevant to Visible Lasers. Boness, M. J. and Hyman, H. A. AERL Semi-Annual Report Sept 1976 - Feb 1977.

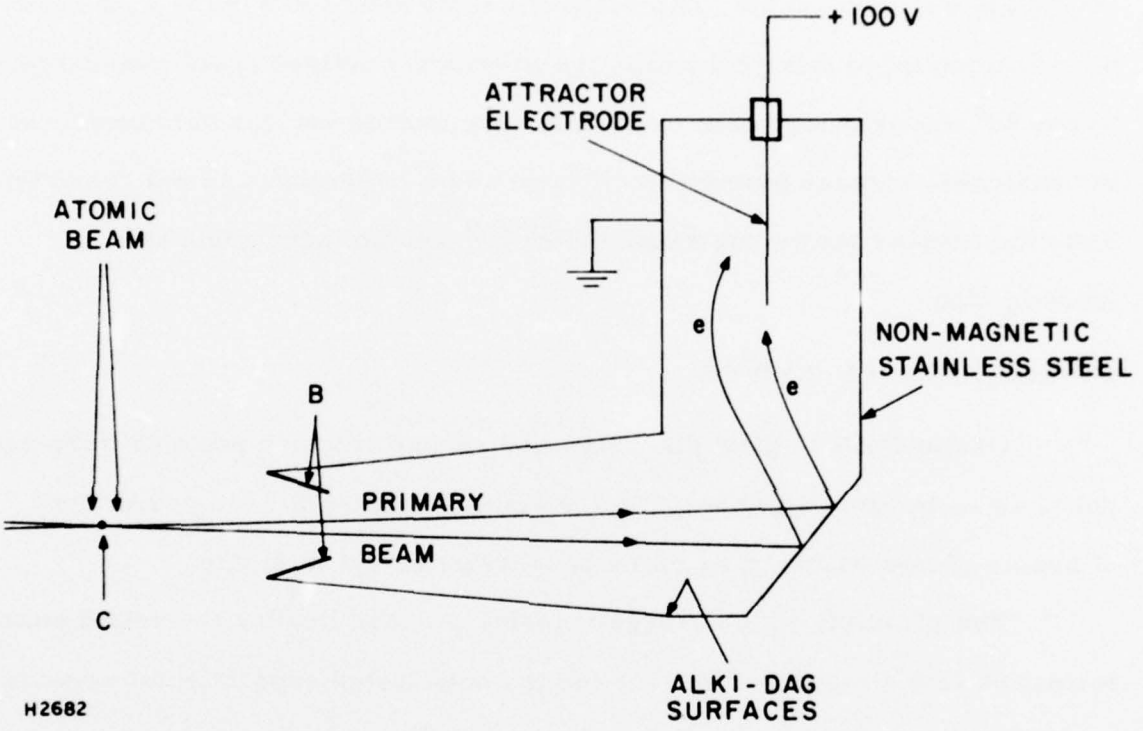

Figure 3 Schematic of the Cross Section of the Primary Beam Collector

surfaces after the beam had traversed the collison region. Since the primary beam intensity was ~1 μA and the objective was to reduce the strong scattered background to less than 1 cps on attenuation of thirteen orders of magnitude was necessary! The beam collector shown in Figure 3 successfully accomplished this goal within the previously defined scattering range. Below 20^{o} the primary beam physically encountered various components of the analyzer entrance optics and efficient beam collection was not possible. Thus the angular scattering range below 20^{o} was not accessible to investigation.

B. METASTABLE SOURCE

Originally both glow discharge and charge transfer sources were proposed as techniques which might offer viable schemes for the production of beams of metastable rare gases possessing useful intensity.

The principle of the charge transfer process leading to excited state formation is indicated in Figure 4 and the anticipated experimental arrangement is shown in Figure 5.

Charge exchange cross sections for collisions between rare gas ions and alkali metals are known to exhibit extremely large cross sections.[12] Since the alkali metal ionization potential is near resonant with the ionization potential of the corresponding metastable rare gas then it is to be expected, and has in fact been confirmed[13] that these charge exchange collisions are likely to produce copious amounts of metastable states of the rare gas.

---

12. Peterson, J. R. and Lorentz, D. C. Phys. Rev. 182, 152 (1969).
13. Neynaber, R. H. and Magnuson, G. D., J. Chem. Phys. 65, 5239 (1976).

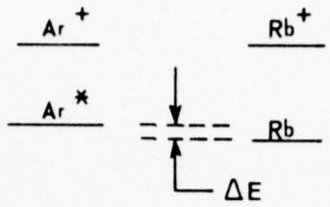

Ar

$$Ar^+ + Rb \longrightarrow Rb^+ + \begin{cases} Ar^* \\ Ar \end{cases}$$

$$\sigma \sim 1.5 \times 10^{-14}\ cm^2$$

(J.R. PETERSON & D.C. LORENTS, PHYS REV, 182, 152, (1969))

BRANCHING RATIOS, γ

RARE GAS X	ALKALI	$\gamma = \frac{X^*}{X + X^*}$
He	Cs	0.85
Ne	Na	0.5
Ar	Rb	0.4

(R.H. NEYNABER & G.D. MAGNUSON, J. CHEM. PHYS. 65, 5239, (1976))

G7785

Figure 4 Charge Exchange Leading to Excited State Formation

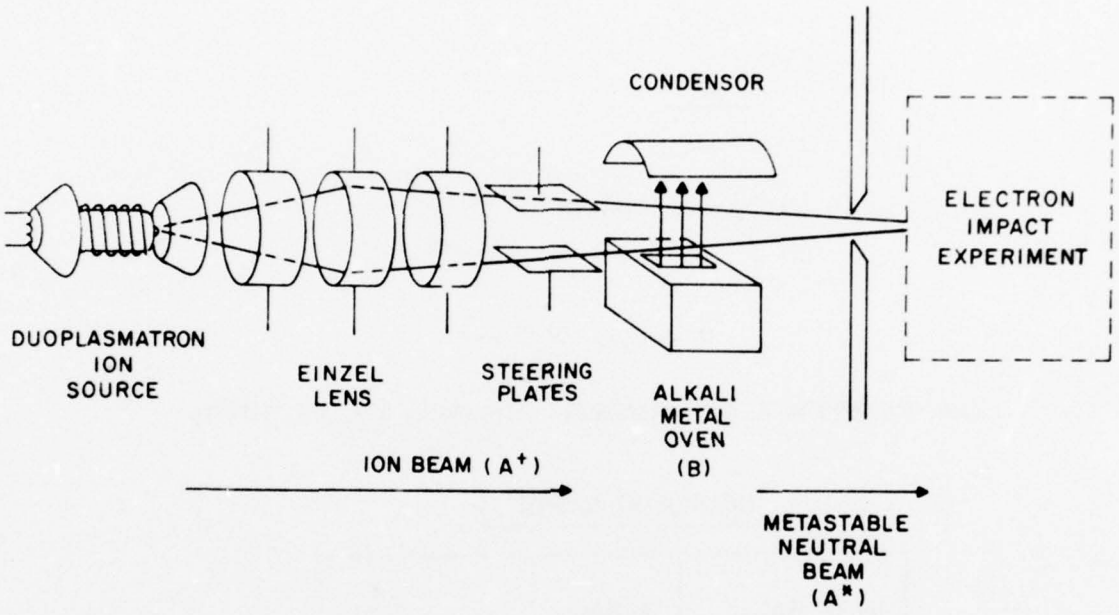

Figure 5 Schematic of the Charge Exchange Apparatus for Metastable Rare Gas Production

Both the charge transfer and glow discharge techniques were pursued initially, however, the relative technical simplicity of the glow discharge technique has led to faster development of this source to the extent that an optimized design has been installed in the system in order to attempt electron scattering experiments.

Glow Discharge Source

The principle of the glow discharge source is to simply create a low pressure stable DC discharge and to allow the discharge products to effuse from a small aperture located at the end of the discharge tube. The discharge tube is located in a separately pumped chamber having a pumping speed of $\sim 550^{o}$ ℓ/sec. This chamber communicates with the spectrometer chamber via a 0.050" diameter orifice. Various apertures can be placed between the discharge tube orifice and the 0.050" orifice separating the two chambers. Bias potentials can be applied to these apertures in order to reject charged particles and to quench high lying, long lived Rydberg states in the beam. Thus in principle it is possible to extract a quasi - atomic beam through the 0.050" aperture which contains only ground state atoms and the required metastable atoms.

One of the early designs of discharge tube is illustrated in Figure 6. The particular source shown was a modified He - Ne discharge laser tube. The original tube was terminated close to the inner capillary section and sealed with a glass plate carrying a 0.020" diam hole.

The performance of the various sources was assessed by placing an Auger detector $\sim$10 cm downstream of the source. The main components of the detector and the operating circuit are shown in Figure 7.

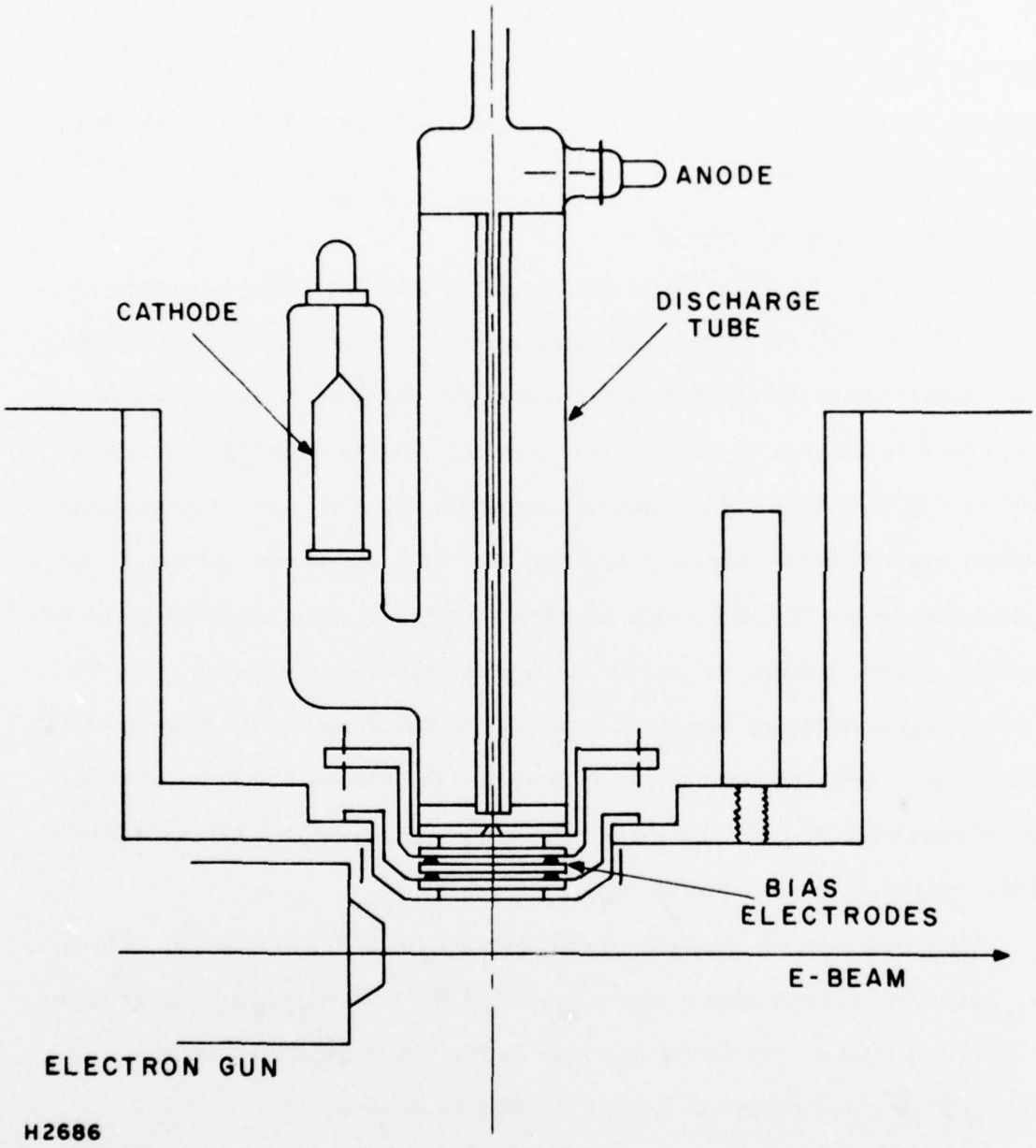

Figure 6 Schematic of an Early Design of Glow Discharge Metastable Source

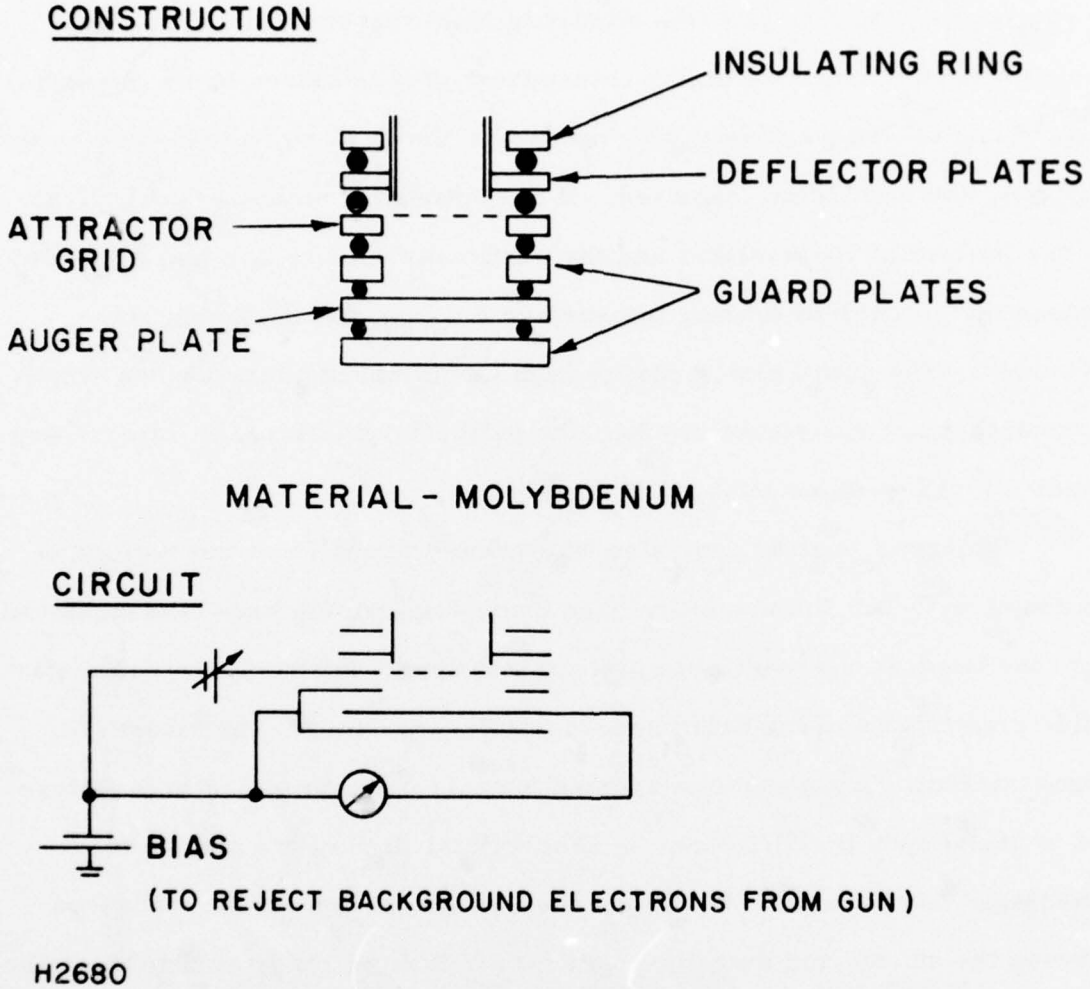

Figure 7 Schematic of the Auger Detector and Operating Circuit

The detector operates on the Auger principle, namely that metastable atoms possessing excitation energy in excess of the work function of a metal surface may liberate electrons from that metal surface upon impact with it. Usually a highly transparent grid is placed above the metal surface and biased positively with respect to the surface so that the ejected electrons are completely removed. If the secondary emission coefficient for the particular meatastable and the particular surface are known then by measuring the current leaving the surface the metastable flux can be estimated. The guard plates ensure high electrical insulation since small currents are normally encountered, the deflector plates are to remove any remaining charged particles from the beam.

Energetic photons may also liberate electrons from the surface of the Auger detector and therefore once charged particles have been removed from the beam it is essential to discriminate between the photon and metastable components of the beam both of which contribute to the measured Auger current. The technique adopted for this purpose is due to Stebbings[14] and is based upon the difference in absorption length of the photon and metastable components of the beam when a background gas is introduced between the source and detector. Much of Stebbings reported data described the absorption of metastable helium atoms and photons produced in a low pressure helium discharge by argon gas contained in a gas cell between the source and detector. Therefore for comparative purposes the performance of the various discharge tubes was usually determined initially by operating with a helium discharge and performing attenuation measurements of the

14. Stebbings, R. F., Proc. Roy. Soc. 241, 270 (1957).

with a helium discharge and performing attenuation measurements of the photon/metastable beam at the Auger detector as a function of argon background gas pressure which could be separately and uniformly introduced into the path of the beam via an auxilliary gas inlet in the spectrometer chamber. Not surprisingly the discharge source illustrated in Figure 6 possessed an extremely large photon to metastable ratio, so much so that exact measurement of the metastable component was extremely difficult. The efficient photon production was probably due to a combination of discharge length and the capillary section which acted as a very efficient light pipe.

A variety of discharge sources were investigated and the final design adopted is shown in Figure 8. The source consists of a short discharge tube approximately two inches long which is closed at one end by a glass plate carrying a 0.020" diam hole. The discharge anode was placed beyond the end of the 0.020 aperature so that the discharge was constricted by the 0.020" aperature prior to reaching the anode. This constriction was found to be key feature for optimizing metastable production. Maintaining a short discharge length was found to reduce the photon component.

Initially sputtering from the cathode was found to severely limit the operating lifetime of the discharge tube. By using high purity nickel for the cathode material combined with the mounting arrangement shown in Figure 8 this problem was eventually eliminated. The important feature of the cathode design was to avoid hot spots by carefully shielding edges of the cathode and by ensuring that the discharge uniformly covers the interior surface of the cathode.

A typical plot of current measured at the Auger detector vs background pressure is shown in Figure 9. This plot is for a helium discharge using argon as the background gas. Two regimes are clearly discernible

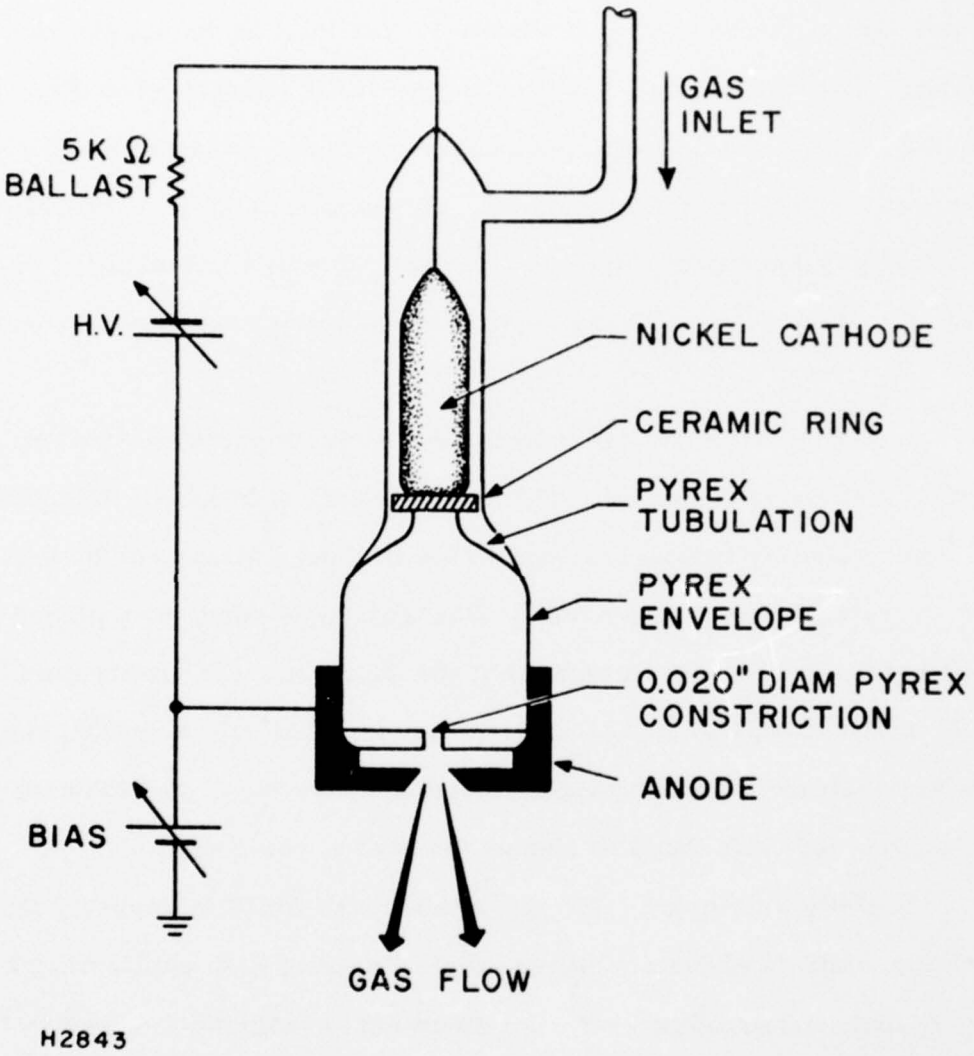

Figure 8 Schematic of the Final Optimized Design of Discharge Tube

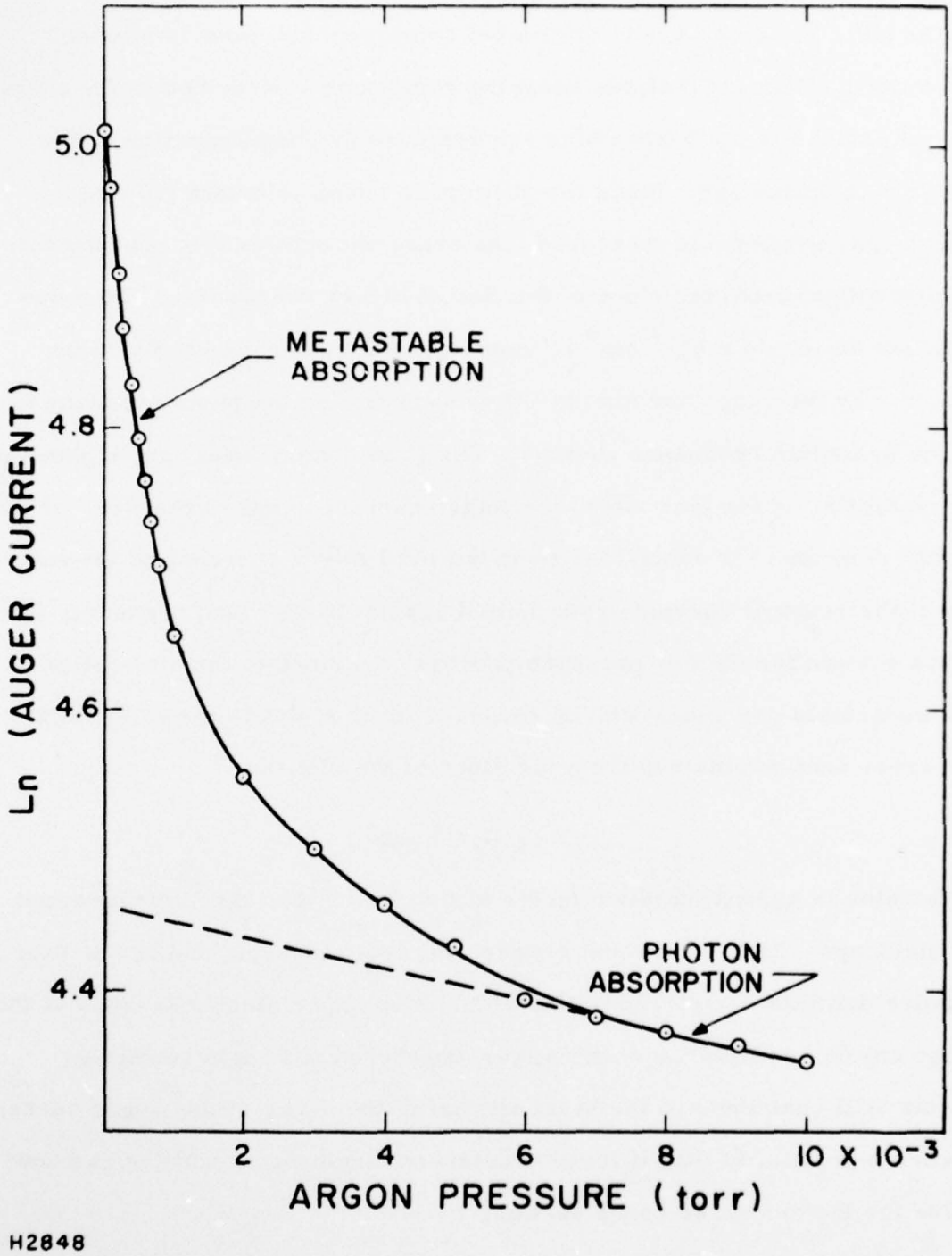

Figure 9 Plot of ℓn Auger Detector Current vs Pressure for a Helium Discharge Using Argon as the Background Gas

on the plot, an early rapidly attenuated component followed by a much larger tail. The more slowly decaying component is ascribed to the absorption of photons in the beam which are removed by photoionization of the argon background gas. Since the absorption length is known (10 cm) and the gas pressure is measured, the cross section for this process can be determined from the slope of the line at higher pressures. The value obtained viz $\sigma = 4 \times 10^{-7}$ cm^2 is in excellent agreement with the value obtained by Stebbings and also by other workers for the photoionization of argon by helium resonance photons. The photon component can be obtained by extrapolating the long tail of the Auger current to zero pressure. If the photon component is subtracted from the total Auger current and the natural log of the residual current again plotted against background pressure, the cross section for the low pressure process, ascribed to the attenuation of the metastable component can be deduced. Such a plot is shown in Figure 10, the cross section obtained from the slope of the plot is

$$\sigma = 5 \times 10^{-15} \text{ cm}^2$$

This value is approximately a factor of five lower than the value obtained by Stebbings. This is of some concern but could be explained by the poor angular definition employed in this attenuation experiment. Because of the large angular acceptance of the Auger detector small angle scattering events still contribute to the beam and hence the decay of the Auger current occurs more slowly than if these events were included, resulting in a low value for the measured cross section.

These measurements were performed as a function of discharge current and discharge pressure in order to optimize the metastable

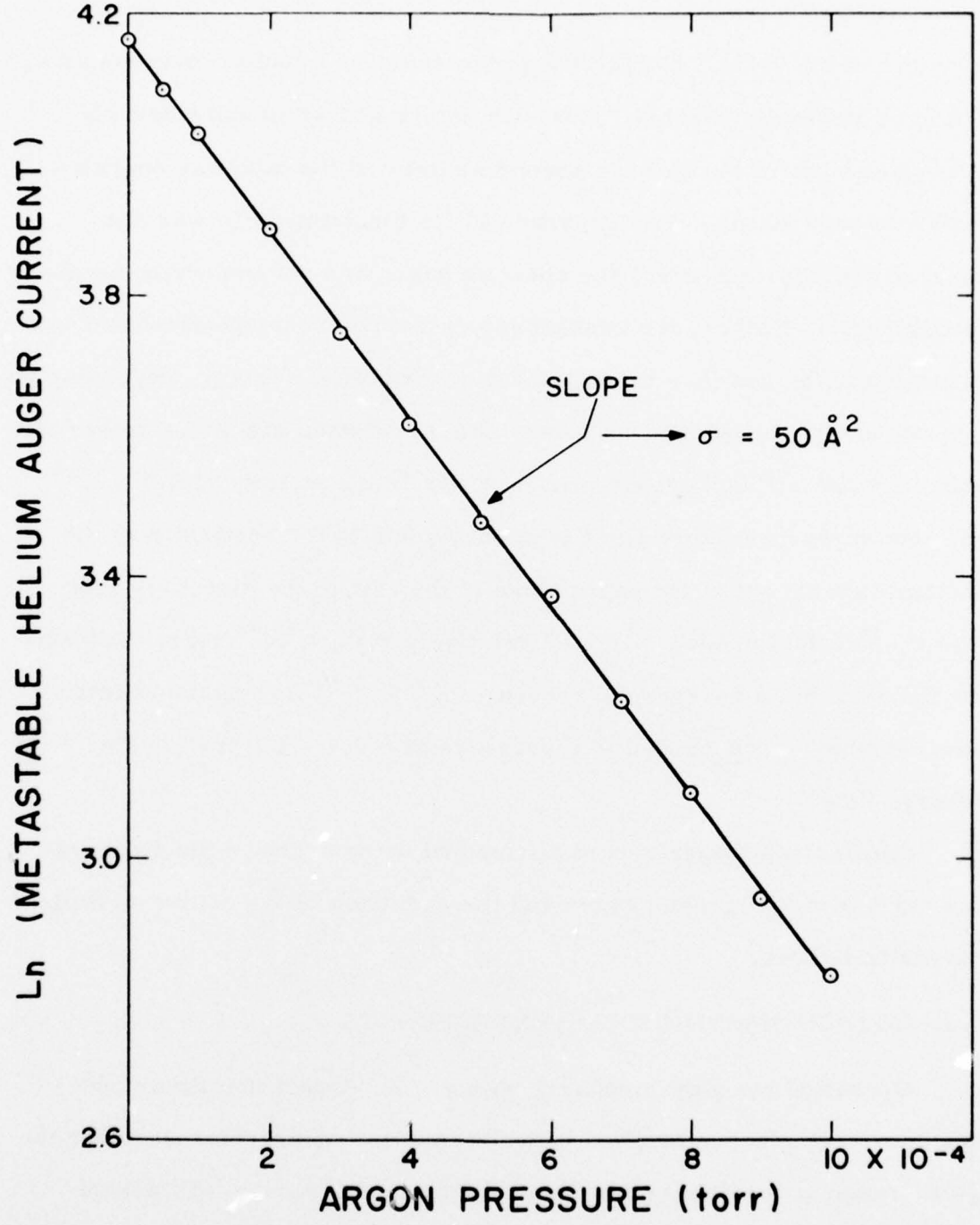

Figure 10 Plot of ℓn Auger Current Minus Photon Components vs Background Pressure

component of the beam. Metastable production was found to increase as a function of discharge current. However, thermal loading considerably shortened the life of the cathode beyond 40 mA and the tube was operated typically around 30 mA. The pressure in the discharge tube was not measured directly, however, the absolute value was not important for these measurements. Rather, the background pressure in the spectrometer was measured and the gas flow through the discharge tube varied. Depending on the particular gas employed the metastable production reached a rather flat maximum when the background pressure was in the vicinity of $2\text{-}3 \times 10^{-6}$ torr. The higher pressure limit is probably due to the scattering of the metastable atoms out of the beam close to the exit of the discharge tube where the residual pressure is still relatively high, $\approx 10^{-3}$ torr. Calculations indicate that a background pressure of 2×10^{-6} torr in the spectrometer chamber corresponded to a pressure of $\sim 0.1 - 1.0$ torr in the discharge tube.

Similar experiments were performed using argon in the discharge and a variety of background gases and the operation of the source optimized as described above.

C. ELECTRON SPECTROSCOPY EXPERIMENTS

Operating the glow discharge with argon, experiments were performed according to the original conception of the measurement. Over the angular range accessible to the experiment and at a variety of incident electron energies no measurable electron-metastable scattering energy loss signals in the vicinity of 1.6 eV were detected. Signal averaging practices were routinely employed, the averaging interval being determined by the various factors governing the long term stability of the experiment.

Assuming a cross section for the electron-metastable scattering cross section of 10^{-14} cm^2 and assuming that the angular distribution is isotropic, the calculations indicate that assuming a metastable density of 10^7 cm^{-3} then the electron scattering signal from the metastable argon atoms should be on the order 5 cps. The experimental signal-to-noise ratio combined with the signal averaging intervals available as determined by stability considerations should have permitted such a signal to be detected. Since it was not, one possible explanation for this result might be the assumption pertaining to the isotropic nature of the angular distribution which was invoked in order to perform the scattering calculation.

The transition

$$Ar\,(4sj) + e \rightarrow Ar\,(4pj') + e$$

is of course a strongly allowed optical transition. It is well known that at high electron energies angular distributions for the scattered electrons are strongly peaked in the forward direction. At low energies generalizations are more difficult and several factors such as resonance phenomena and the limited number of partial wave contributions to the scattering amplitude complicate the issue tremendously. Thus the non-isotropic behavior of the angular distribution could be a valid explanation for the absence of the scattered electron signal over the angular range accessible to the experiment.

D. THE FLUORESCENCE TECHNIQUE

Due to the problems encountered with the technique of energy loss spectroscopy the possibility of a fluorescence measurement was considered as a method of observing the process of interest,

$$e + Ar^{*}(4sj) \rightarrow Ar^{**}(4pj') + e$$

via the fluorescence

$$Ar^{**}(4pj') \rightarrow Ar^{*}(4sj) + h\nu$$

A comparison of the relative sensitivities of the fluorescence technique and the method of energy loss spectroscopy involves many factors. The near isotropic nature of the fluorescence emission together with the possibility of employing large f number extraction optics strongly favors the fluorescence technique. However, detector sensitivity, intrinsic noise, and spectrometer transmission efficiency favor the energy loss spectroscopy. After considering each of these factors it appeared that the fluorescence technique might provide a better opportunity to perform this particular measurement.

An additional benefit accrued from adopting the fluorescence technique was the possibility to increase the incident electron beam intensity by using larger apertures in the diode stage of the gun. This improvement was not possible when employing the electron spectrometer since the corresponding increase in the angular divergence and space charge spreading of the electron beam generated more problems than benefits.

Once the decision was taken to adopt the fluorescence technique the experiment was modified accordingly. A schematic of the fluorescence diagnostic arrangement is shown in Figure 11. Rather than employ an

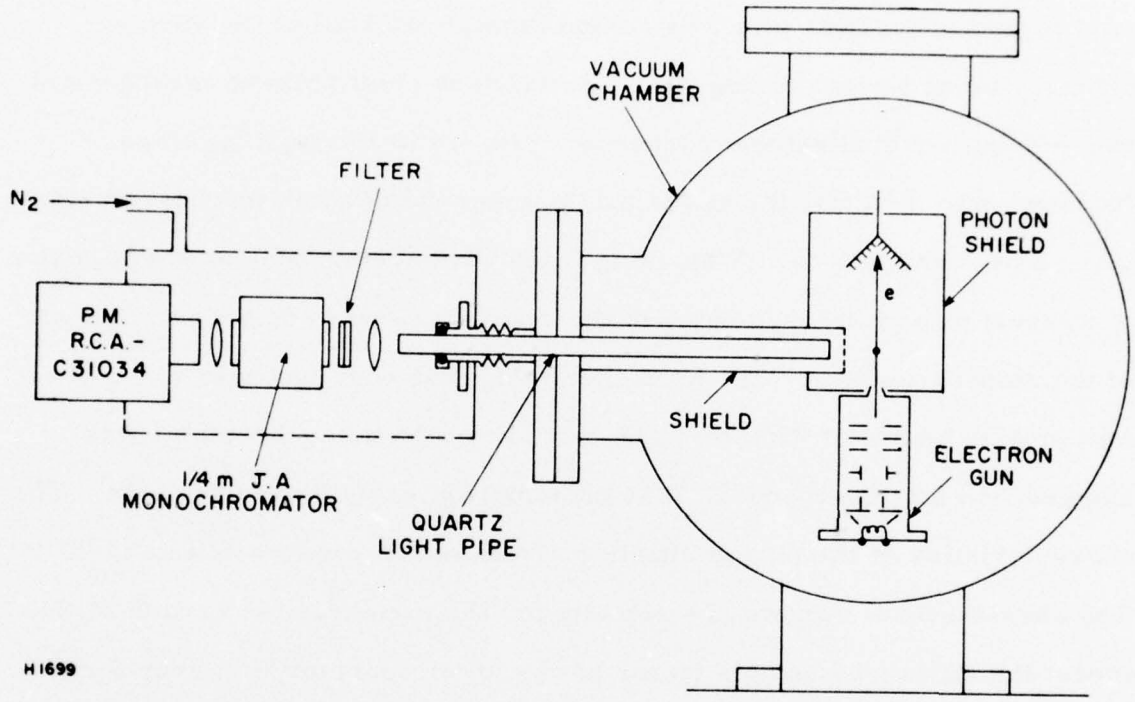

Figure 11 Schematic of the Fluorescence Diagnostic Arrangement

optical extraction system comprised of lenses which requires careful alignment a light pipe system was employed as shown. The light pipe was 3/8" diameter quartz and subtended approximately an f1 ratio at the collision region. The light pipe was sealed through the wall of the vacuum chamber using a viton o-ring seal. A stainless steel bellows arrangement was employed for alignment purposes. The end of the light pipe was focussed onto the entrance slit of a 1/4-meter Jarrel-Ash monochromator using a cylindrical lens. A blocking filter which defined the spectral region of interest was interposed between the cylindrical lens and the entrance slit of the monochromator. The monochromator was equipped with a 590 lines/mm grating blazed at 750 nm. The exit slit of the monochromator was coupled into an RCA model C31034 photomultiplier using another lens. The characteristics of the photomultiplier are shown in Figures 12(a) and (b). The characteristics shown are actually for the improved 'A' variant of this model the difference being a factor of two lower quantum efficiency for the C31034 model. In order to reduce the dark count the tube was housed in a refrigerated housing and cooled to -20°C. At this temperature a dark count rate of approximately 20 cps was obtained. The refrigerated housing contained a built-in pulse preamplifier the output of which was taken to the standard Canberra Industries pulse counting equipment previously described.

E. FLUORESCENCE EXPERIMENTS

The experimental arrangement finally employed for the fluorescence measurements is shown in Figure 13.

As with the energy loss spectroscopy considerable problems were encountered with background noise signals originating in the experiment

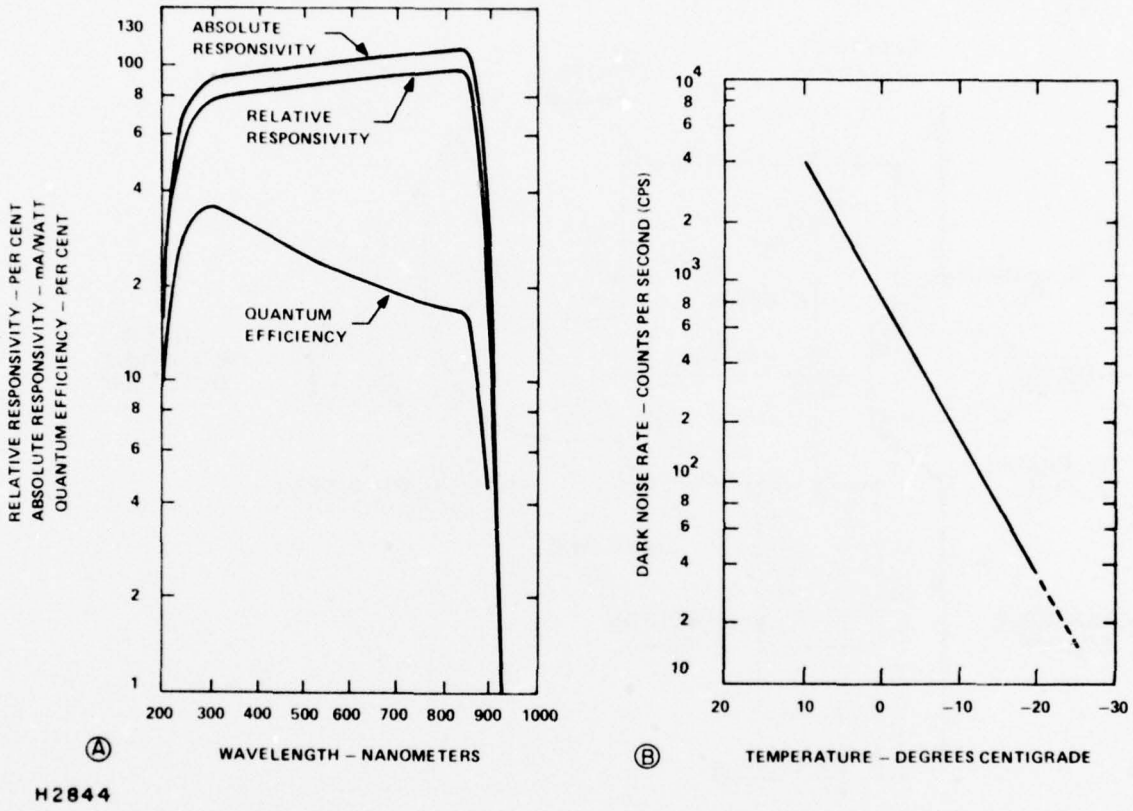

Figure 12(a) Typical Photocathode Spectral Responsivity Characteristics of the RCA Model C31034A Photomultiplier

(b) Typical Dark Noise Rate as a Function of Temperature

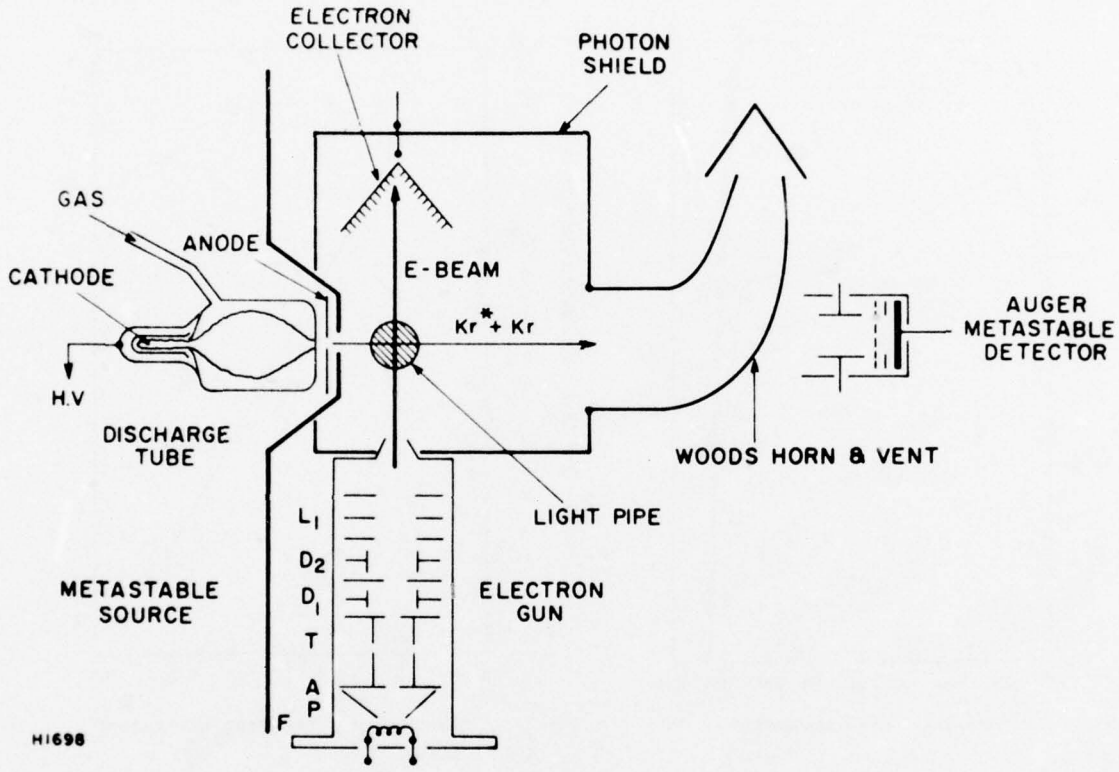

Figure 13 Schematic of the Experimental Arrangement Employed for the Fluorescence Measurement

itself. The photon background generated by the discharge overlapped exactly the fluorescence signals of interest and was extremely difficult to cope with. The signal was reduced as much as possible by introducing a complete shield around the collision region as shown and by collecting the major component of the photon flux inside the Woods' Horn which was open at the small end in order to vent the box.

Photons emitted from the filament which travelled collinearly through the collision region with the electron beam and then scattered off various surfaces into the collection optics were another problem. This was reduced considerably by providing the venetian blind style electron collector which both monitored the primary electron beam and provided a dump for the continuum emission from the filament.

Initially experiments were performed to measure the Ar (4pj') → Ar (4sj') fluorescence by exciting the 4pj' levels directly by electron collisions with ground state Ar atoms. This served to verify the performance of the system and also to provide a convenient method of exactly calibrating the monochromator reading for the wavelengths of interest. Naturally the discharge was unnecessary for these experiments the primary electron beam was simply crossed with a beam of ground state argon atoms. Fluorescence spectra for the transitions of interest in argon and krypton obtained at an incident electron energy of approximately 20 eV are shown in Figures 14 and 15 respectively.

Experiments are now in progress to measure the 4 pj' → 4sj' fluorescence emission excited by electron collisions with metastable argon atoms.

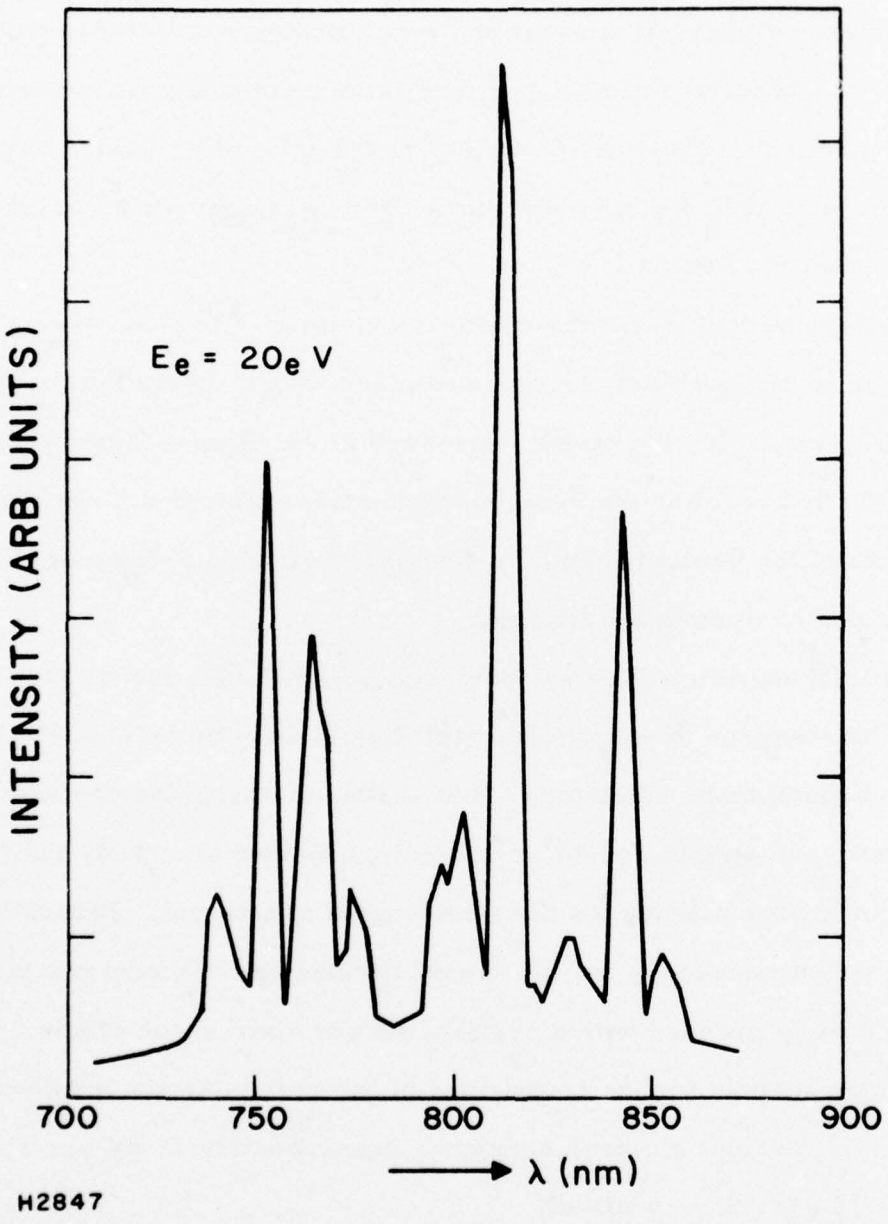

Figure 14 Fluorescence Spectrum for the Argon Ar (4pj') → Ar (4sj) Transitions Obtained at an Electron Energy of 20 eV

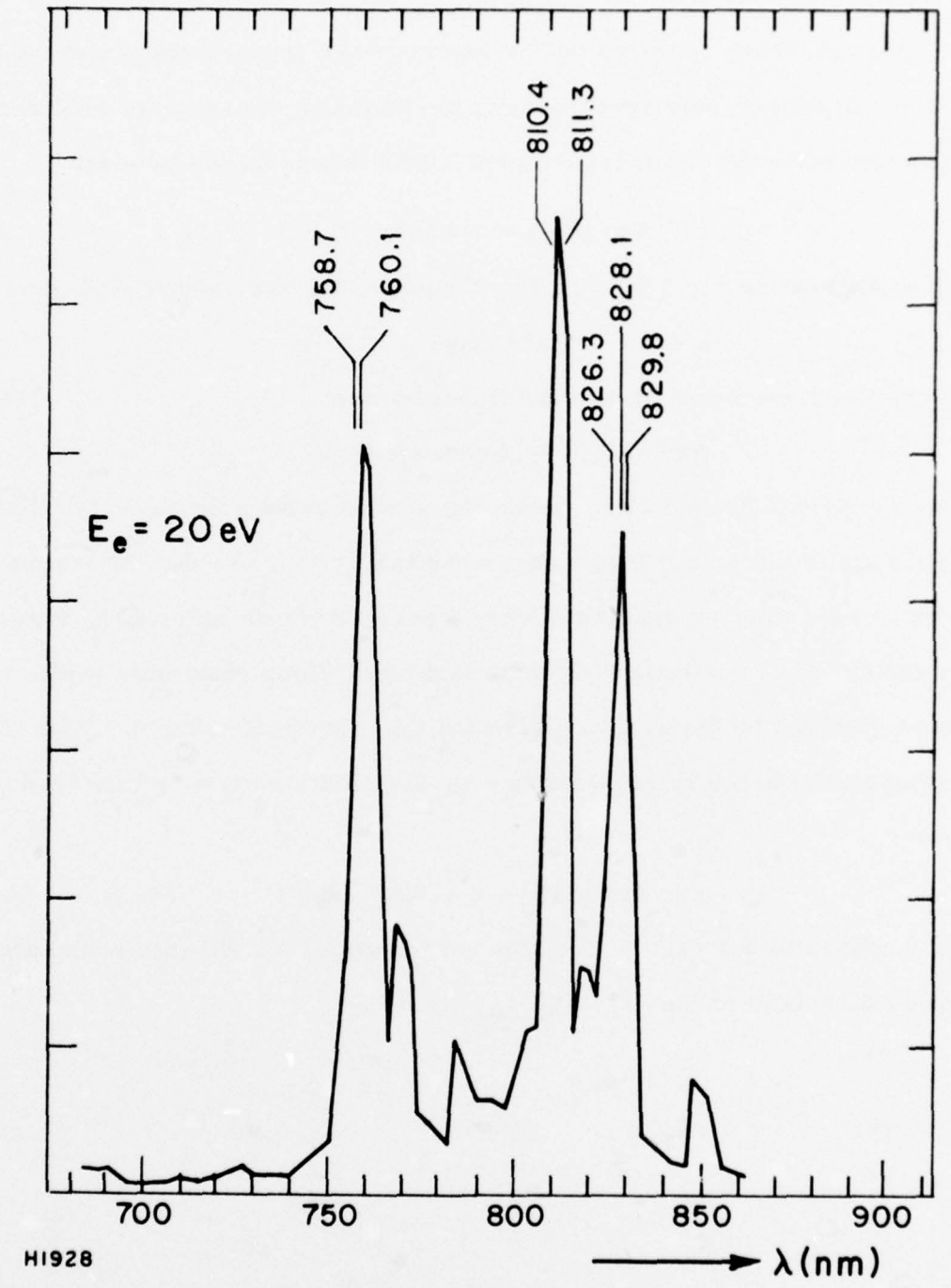

Figure 15 Fluorescence Spectra for the Krypton Kr (5pj') → Kr (5pj) Transitions Obtained at an Electron Energy of 20 eV

One limitation imposed by the fluorescence measurement and not shared by the energy loss spectroscopy technique is the range of electron energies available for the measurement. The threshold for process

$$e + Ar^{*}(4sj) \rightarrow e + Ar^{**}(4pj')$$

occurs at approximately 1.6 eV. The threshold for the ground state process

$$e + Ar \rightarrow Ar^{**}(4pj)$$

with consequent emission of similar fluorescence

$$Ar^{**}(4pj') \rightarrow Ar^{*}(rsj) + h\nu$$

occurs at approximately 13 ev. Since the ground state atoms are far more numerous than metastable atoms then even taking into account the favorable excitation cross section ratio the fluorescence emission originating from direct ground state excitation to the 4p level will completely overwhelm the emission obtained by electron impact with the metastable atoms. Therefore depending on the primary electron energy distribution, measurements for the process

$$e + Ar^{*}(4sj) \rightarrow e + Ar^{**}(4pj')$$

will be confined to the region from the threshold for the direct ground state excitation threshold to the 4pj' levels, ~13 eV.

III. THEORY

In the previous Semi-Annual Report[15] we have given the formulas required for calculating the cross sections, together with the eigenvalues (scaling parameters) of the radial Schrodinger equation. The corresponding eigenfunctions have been used to compute the cross sections, and the results will be given in this section.

In Figures 16 and 17 are shown the relevant energy levels of excited argon and krypton. In intermediate coupling which is the appropriate representation for the excited rare gases, only the total angular momentum, J and parity of the state are good quantum numbers. To the left of the two figures are the levels of the two most important configurations, Ar* (4s, 4p) and Kr* (5s, 5p), labelled by their total J-values (the commonly-used Paschen notation[16] has also been included). The J = 2 ($1s_5$) and J = 0 ($1s_3$) levels are metastable, while the J = 1 ($1s_2$, $1s_4$) levels can radiatively decay to the ground state. However, under typical laser operating conditions, the two J = 1 states are optically trapped and therefore effectively long-lived. Electron impact excitation of the J = 1 levels is therefore also of importance. To the right in each figure we have indicated the statistically-averaged energy level of each configuration, denoted by the orbital ($n\ell$) of the active electron (the core configurations are given at the bottom).

---

15. Boness, M.J.W. and Hyman, H.A., Investigation of Electron Impact Processes Relevant to Visible Lasers, Semi-Annual Report, Sept. 1, 1976 to Feb. 28, 1977.

16. Moore, C.E., Atomic Energy Levels, Vols. I and II, Circular of the National Bureau of Standards 467, U.S. Dept. of Commerce, Washington, D.C. (1949).

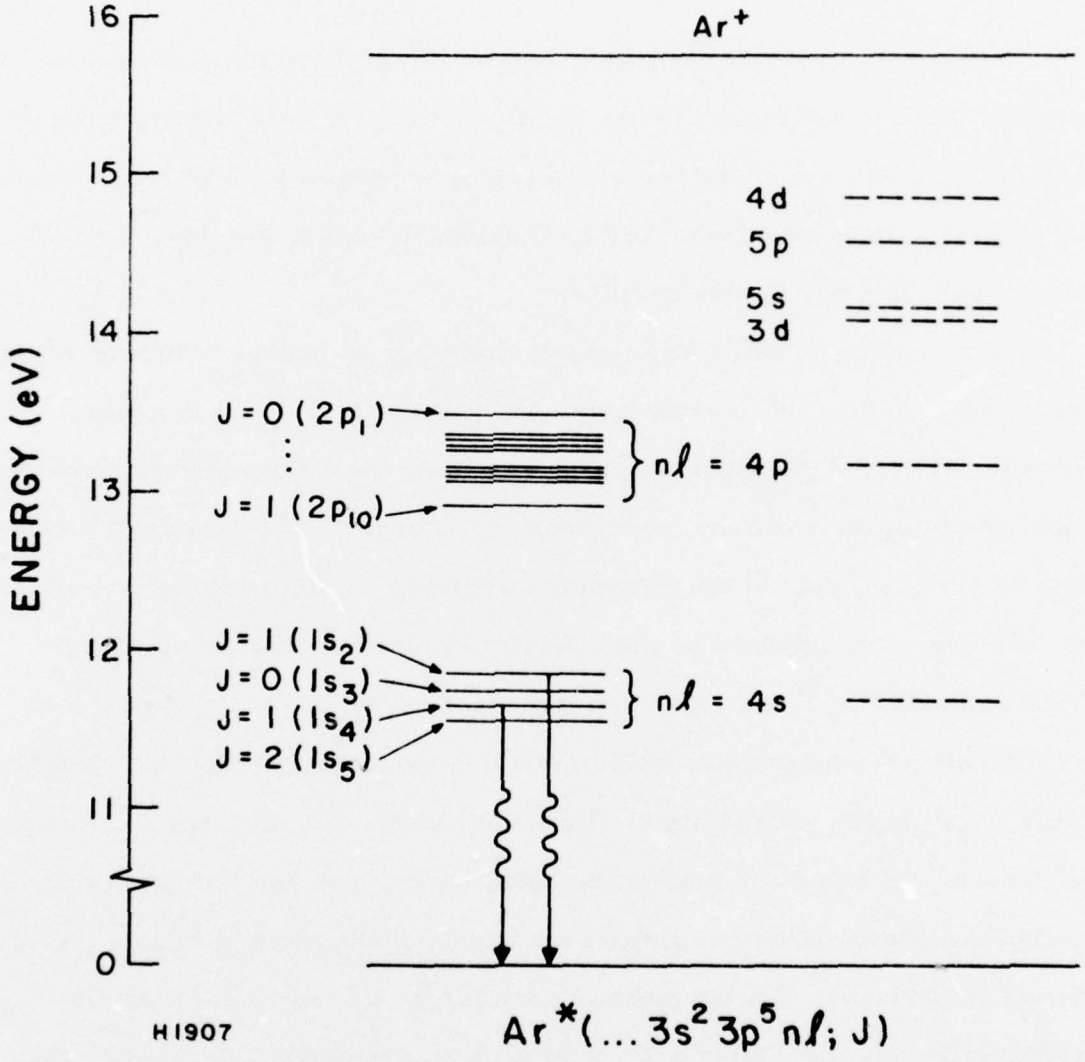

Figure 16 Energy Level Diagram for Excited States of Argon

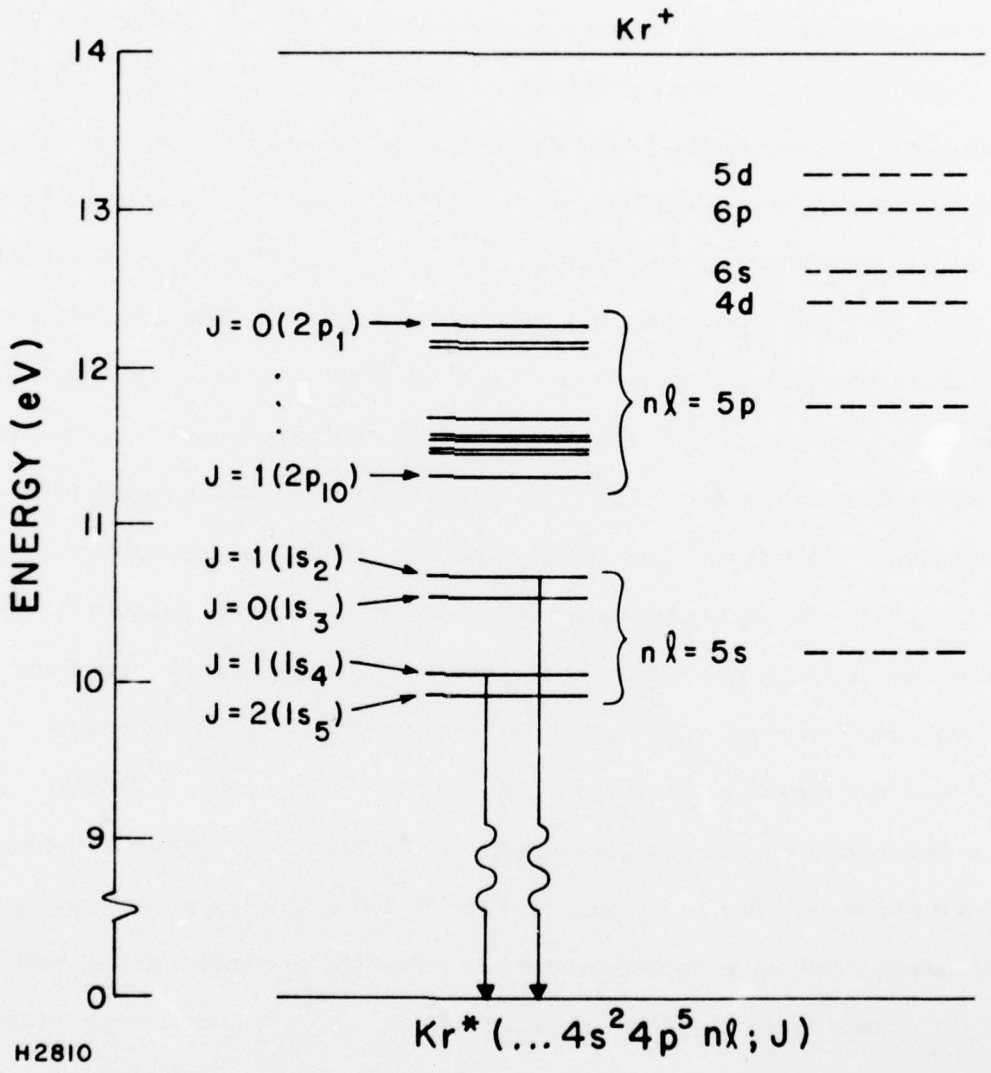

Figure 17 Energy Level Diagram for Excited States of Krypton

Born cross sections have been calculated in the intermediate coupling representation for the transition arrays Ar* (4s; J → 4p; J') and Kr* (5s; J → 5p; J'), and the results are summarized in Table 1 - 4. The initial- and final-state notation refers to the energy levels to the left of Figures 16 and 17. Table 1 lists the cross sections, at several electron impact energies of interest, for excitation of the argon metastable states ($1s_5$ and $1s_3$) to all levels of the 4p configuration, while Table 2 gives the cross sections from the argon optically-trapped states ($1s_4$ and $1s_2$) to all of the 4p states. Tables 3 and 4 list the corresponding results for krypton. The final states marked with an asterisk indicate those transitions which are completely forbidden in jK-coupling,[17] which is the best of the pure coupling schemes for excited argon and krypton. Clearly, not all of the cross sections for these "forbidden" transitions are small, and this points out the need for using the proper coupling representation to obtain meaningful results.

Effective or average Born cross sections [defined as the sum over final J-states and average over initial J-states (see Ref. 15)] have been computed for the transitions Ar* (4s → nℓ) and Kr* (5s → nℓ), with the notation referring to the energy level scale to the right of Figures 18 and 19. It is clear that the Ar* (4s → 4p) and Kr* (5s → 5p) transitions are dominant. For these cases, the Born approximation is expected to considerably overestimate the cross section at low energies due to the very long-range nature of the dipole coupling potential. We have therefore used a method due to Seaton,[18] which is essentially a Unitarized Impact Parameter Born (UIPB)

---

17. Cowan, R. D. and Andrew, K. L., J. Opt. Soc. Amer. 55, 502 (1965).
18. Seaton, M. J., Proc. Phys. Soc. 79, 1105 (1962).

TABLE 1. ARGON CROSS SECTIONS

Initial State	Final State	Cross Section (πa_o^2) E_i = 5 eV	E_i = 10 eV	E_i = 15 eV
$1s_5$	2_{p10}	2.99(1)†	2.03(1)	1.56(1)
	2_{p9}	8.76(1)	6.16(1)	4.78(1)
	2_{p8}	1.69(1)	1.20(1)	9.29
	2_{p7}	4.80	3.43	2.68
	2_{p6}	3.63(1)	2.60(1)	2.04(1)
	2_{p4}*	8.18(-1)	6.01(-1)	4.74(-1)
	2_{p3}*	5.70	4.21	3.32
	2_{p2}*	5.02	3.72	2.94
$1s_3$	2_{p10}*	1.30(1)	8.53	6.47
	2_{p7}*	2.24(1)	1.54(1)	1.19(1)
	2_{p4}	9.82(1)	6.95(1)	5.40(1)
	2_{p2}	5.32(1)	3.80(1)	2.97(1)

* Forbidden in jK-coupling.

† The number in parentheses indicates the power of ten by which each entry should be multiplied.

TABLE 2. ARGON CROSS SECTIONS

Initial State	Final Stage	Cross Section (πa_o^2) E_i = 5 eV	E_i = 10 eV	E_i = 15 eV
$1s_4$	2_{p10}	1.68(1)†	1.13(1)	8.61
	2_{p8}	7.30(1)	5.08(1)	3.92(1)
	2_{p7}	4.54(1)	3.19(1)	2.48(1)
	2_{p6}	1.35(1)	9.52	7.40
	2_{p5}	1.91(1)	1.38(1)	1.08(1)
	2_{p4}*	4.56(-1)	3.29(-1)	2.58(-1)
	2_{p3}*	1.83(1)	1.32(1)	1.04(1)
	2_{p2}*	2.15	1.57	1.23
	2_{p1}*	1.04(-2)	7.89(-3)	6.28(-3)
$1s_2$	2_{p10}*	1.26	8.15(-1)	6.14(-1)
	2_{p8}*	6.73	4.49	3.42
	2_{p7}*	2.02	1.36	1.04
	2_{p6}*	2.94(1)	1.99(1)	1.53(1)
	2_{p5}*	1.49(-2)	1.03(-2)	7.95(-3)
	2_{p4}	2.85(1)	1.97(1)	1.52(1)
	2_{p3}	7.59(1)	5.28(1)	4.08(1)
	2_{p2}	3.36(1)	2.35(1)	1.82(1)
	2_{p1}	1.91(1)	1.38(1)	1.08(1)

* Forbidden in jK-coupling.

† The number in parentheses indicates the power of ten by which each entry should be multiplied.

TABLE 3. KRYPTON CROSS SECTIONS

Initial State	Final State	Cross Section (πa_o^2) E_i = 5 eV	E_i = 10 eV	E_i = 15 eV
$1s_5$	$2p_{10}$	3.56(1)†	2.46(1)	1.90(1)
	$2p_9$	8.83(1)	6.27(1)	3.89(1)
	$2p_8$	1.87(1)	1.32(1)	1.04(1)
	$2p_7$	4.37	3.16	2.48
	$2p_6$	4.08(1)	2.96(1)	2.33(1)
	$2p_3$*	6.58(-1)	5.58(-1)	4.60(-1)
	$2p_2$*	6.35(-1)	5.39(-1)	4.45(-1)
$1s_3$	$2p_{10}$*	4.19	2.57	1.90
	$2p_7$*	1.06	6.73(-1)	5.04(-1)
	$2p_4$	9.30(1)	6.62(1)	5.17(1)
	$2p_3$	8.92(1)	6.40(1)	5.01(1)

* Forbidden in jK-coupling.

† The number in parentheses indicates the power of ten by which each entry should be multiplied.

TABLE 4. KRYPTON CROSS SECTIONS

Initial State	Final State	Cross Section (πa_o^2) E_i = 5 eV	E_i = 10 eV	E_i = 15 eV
$1s_4$	$2p_{10}$	1.00(1)†	6.75	5.16
	$2p_8$	7.99(1)	5.54(1)	4.28(1)
	$2p_7$	5.61(1)	3.96(1)	3.08(1)
	$2p_6$	3.01(1)	2.13(1)	1.66(1)
	$2p_7$	1.94(1)	1.41(1)	1.11(1)
	$2p_4$*	1.30(-2)	1.06(-2)	8.60(-3)
	$2p_3$*	6.89(-2)	5.65(-2)	4.61(-2)
	$2p_2$*	1.30	1.06	8.70(-1)
	$2p_1$*	1.09(-2)	9.22(-3)	7.60(-3)
$1s_2$	$2p_{10}$*	1.15	6.97(-1)	5.11(-1)
	$2p_8$*	1.09	6.78(-1)	5.02(-1)
	$2p_7$*	6.89(-1)	4.32(-1)	3.22(-1)
	$2p_6$*	3.15	1.98	1.48
	$2p_5$*	2.65(-2)	1.70(-2)	1.28(-2)
	$2p_4$	3.36(1)	2.35(1)	1.82(1)
	$2p_3$	3.10(1)	2.18(1)	1.70(1)
	$2p_2$	1.05(2)	7.39(1)	5.75(1)
	$2p_1$	1.97(1)	1.43(1)	1.12(1)

* Forbidden in jK-coupling.

† The number in parentheses indicates the power of ten by which each entry should be multiplied.

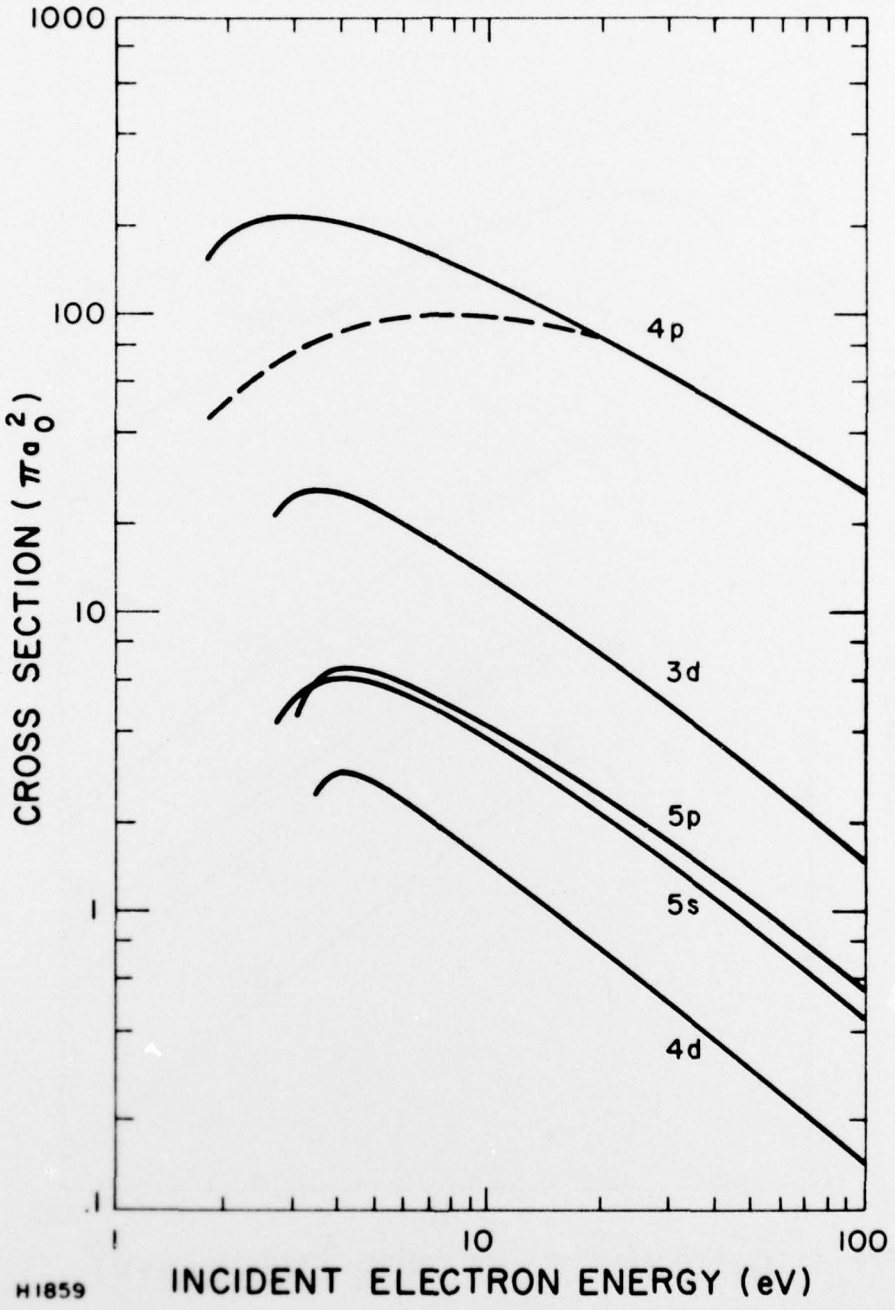

Figure 18 Effective Born Cross Sections for the Transitions Ar*(4s → nℓ). The dashed curve is for the 4s → 4p transition, taking strong-coupling effects into account

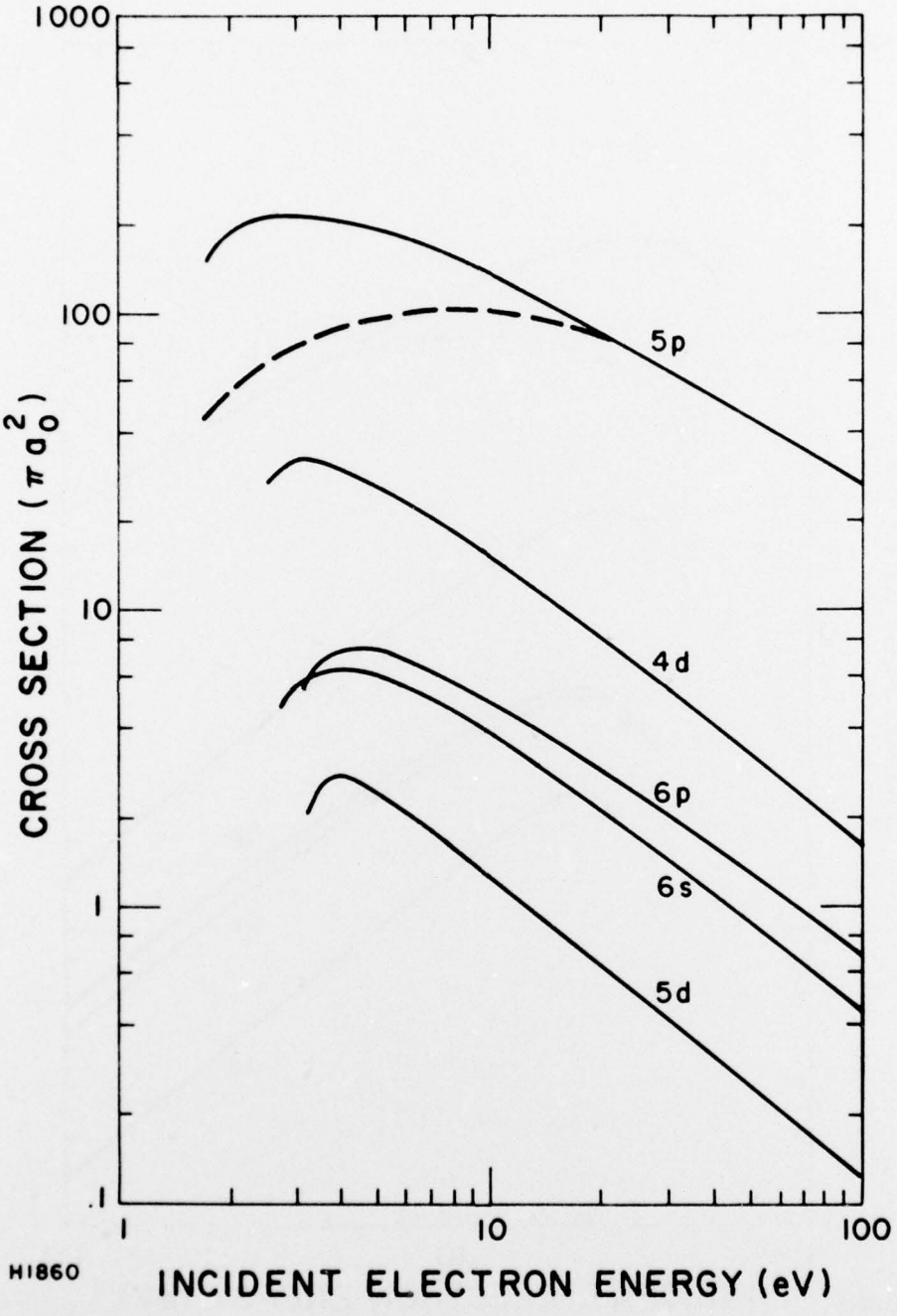

Figure 19 Effective Born Cross Sections for the Transitions Kr* ($5s \rightarrow n\ell$). The dashed curve is for the $5s \rightarrow 5p$ transition, taking strong-coupling effects into account

theory, to estimate the effects of strong coupling. The UIPB results are shown as the dashed curves in Figures 18 and 19. It is obvious that they deviate considerably from the Born approximation, both in magnitude and shape.

To summarize, the principal results of the present investigation are: (1) the electron impact excitation of metastable argon and krypton is dominated by a single transition (4s → 4p for Ar and 5s → 5p for Kr) with a large cross section ($\sim 100\pi\, a_o^2$ at the peak); and (2) strong coupling effects are dominant at low energies for the 4s → 4p and 5s → 5p transitions. In addition, we have shown that a proper choice of coupling scheme is necessary to obtain reasonable results for cross sections between the various substates.

IV. PRESENT STATUS

During this reporting period, after unsuccessful attempts to detect electron scattering from metastable argon atoms using electron spectroscopy the fluorescence technique was substituted for the method of electron energy loss spectroscopy.

The experiment has been modified accordingly and measurements have been performed of fluorescence emission from the transition

$$Ar^{**}(4pj) \rightarrow Ar^{*}(4sj) + h\nu$$

excited by electron collisions with ground state argon atoms. Measurements of the corresponding fluorescence emission in krypton have been performed in a similar manner. A final design of glow discharge tube for metastable production has been adopted and installed in the experiment.

Measurements of the transitions of interest viz

$$e + r^{*}(4sj) \rightarrow e + Ar^{**}(4pj')$$

are currently underway.

REFERENCES

1. "KrF Laser Research," AERL 804, April 1976.

2. Long, D.R. and Geballe, R., Phys. Rev. 1, 260 (1970).

3. Lake, M.L. and Garscadden, A., 28th Gaseous Electronics Conference Rolla, Mo. (1975), Paper C-5.

4. Mityurwa, A.A. and Penkin, N.P., Opt. Spectros. 38, 229 (1975).

5. Wilson, W.G. and Williams, W.L., J. Phys. B9, 423 (1976).

6. Tannen, P.D., "Cumulative Ionization and Excitation of Molecular Nitrogen Metastables by Electronic Impact," Dissertation (1973), School of Engineering, Air Force Institure of Technology.

7. Ewing, J.J. and Brau, C.A., Appl. Phys. Lett. 27, 350 (1975).

8. Ewing, J.J. and Brau, C.A., Phys. Rev. A12, 129 (1975).

9. Mangano, J.A. and Jacob, J.H., App. Phys. Lett. 27, 495 (1975).

10. Investigation of Electron Impact Processes Relevant to Visible Lasers. Boness, M.J. and Hyman, H.A. AERL Semi-Annual Report March-Aug. 1976.

11. Investigation of Electron Impact Processes Relevant to Visible Lasers. Boness, M.J. and Hyman, H.A. AERL Semi-Annual Report Sept 1976 - Feb 1977.

12. Peterson, J.R. and Lorentz, D.C. Phys. Rev. 182, 152 (1969).

13. Neynaber, R.H. and Magnuson, G.D., J. Chem. Phys. 65, 5239 (1976).

14. Stebbings, R.F., Proc. Roy. Soc. 241, 270 (1957).

15. Boness, M.J.W. and Hyman, H.A., Investigation of Electron Impact Processes Relevant to Visible Lasers, Semi-Annual Report, Sept. 1, 1976 to Feb. 28, 1977.

16. Moore, C.E., Atomic Energy Levels, Vols. I and II, Circular of the National Bureau of Standards 467, U.S. Dept. of Commerce, Washington, D.C. (1949).

17. Cowan, R.D. and Andrew, K.L., J. Opt. Soc. Amer. 55, 502 (1965).

18. Seaton, M.J., Proc. Phys. Soc. 79, 1105 (1962).

DISTRIBUTION LIST

Office of Naval Research, Department of the Navy, Arlington, VA 22217 - Attn: Physics Program (3 copies)

Naval Research Laboratory, Department of the Navy, Washington, D.C. 20375 - Attn: Technical Library (1 copy)

Office of the Director of Defense, Research and Engineering, Information Office Library Branch, The Pentagon, Washington, D.C. 20301 (1 copy)

U.S. Army Research Office, Box CM, Duke Station, Durham, N.C. 27706 (1 copy)

Defense Documentation Center, Cameron Station, Alexandria, VA 22314 (12 copies)

Defender Information Analysis Center, Battelle Memorial Institute, 505 King Avenue, Columbus, OH 43201 (1 copy)

Commanding Officer, Office of Naval Research Branch Office, 536 South Clark Street, Chicago, IL 60615 (1 copy)

New York Area Office, Office of Naval Research, 715 Broadway (5th Floor), New York, NY 10003 - Attn: Dr. Irving Rowe (1 copy)

San Francisco Area Office, Office of Naval Research, 760 Market Street, Room 447, San Francisco, CA 94102 (1 copy)

Air Force Office of Scientific Research, Department of the Air Force, Washington, D.C. 22209 (1 copy)

Office of Naval Research Branch Office, 1030 East Green Street, Pasadena, CA 91106 - Attn: Dr. Robert Behringer (1 copy)

Code 102 IP (ONRL), Office of Naval Research, 800 N. Quincy Street, Arlington, VA 22217 (6 copies)

Defense Advanced Research Projects Agency, 1400 Wilson Blvd., Arlington, VA 22209 - Attn: Strategic Technology Office (1 copy)

Office Director of Defense, Research & Engineering, The Pentagon, Washington, D.C. 20301 - Attn: Assistant Director (Space and Advanced Systems) (1 copy)

Office of the Assistant Secretary of Defense, System Analysis (Strategic Programs), Washington, D.C. 20301 - Attn: Mr. Gerald R. McNichols (1 copy)

U.S. Arms Control and Disarmament Agency, Dept. of State Bldg., Rm. 4931, Washington, D.C. 20451 - Attn: Dr. Charles Henkin (1 copy)

Energy Research Development Agency, Division of Military Applications, Washington, D.C. 20545 (1 copy)

National Aeronautics and Space Administration, Lewis Research Center, Cleveland, OH 44135 - Attn: Dr. John W. Dunning, Jr. (1 copy)
(Aerospace Res. Engineer)

National Aeronautics & Space Administration, Code RR, FOB 10B, 600 Independence Ave., SW, Washington, D.C. 20546 (1 copy)

National Aeronautics and Space Administration, Ames Research Center, Moffett Field, CA 94035 - Attn: Dr. Kenneth W. Billman (1 copy)

Department of the Army, Office of the Chief of RD&A, Washington, D.C. 20310 - Attn: DARD-DD (1 copy)
DAMA-WSM-T (1 copy)

Department of the Army, Office of the Deputy Chief of Staff for Operations & Plans, Washington, D.C. 20310 - Attn: DAMO-RQD - (1 copy)

Ballistic Missile Defense Program Office (BMDPO), The Commonwealth Building, 1300 Wilson Blvd., Arlington, VA 22209 - Attn: Mr. Albert J. Bast, Jr. (1 copy)

U.S. Army Missile Command, Research & Development Division, Redstone Arsenal, AL 35809 - Attn: Army High Energy Laser Programs (2 copies)

Commander, Rock Island Arsenal, Rock Island, IL 61201, Attn: SARRI-LR, Mr. J.W. McGarvey (1 copy)

Commanding Officer, U.S. Army Mobility Equipment R&D Center, Ft. Belvoir, VA 22060 - Attn: SMEFB-MW (1 copy)

Commander, U.S. Army Armament Command, Rock Island, IL 61201 - Attn: AMSAR-RDT (1 copy)

Director, Ballistic Missile Defense Advanced Technology Center, P.O. Box 1500, Huntsville AL 35807 - Attn: ATC-O (1 copy)
ACT-T (1 copy)

Commander, U.S. Army Material Command, Alexandria, VA 22304 - Attn: Mr. Paul Chernoff (AMCRD-T) (1 copy)

Commanding General, U.S. Army Munitions Command, Dover, NH 17801 - Attn: Mr. Gilbert F. Chesnov (AMSMU-R) (1 copy)

Director, U.S. Army Ballistics Res. Lab, Aberdeen Proving Ground, MD 21005 - Attn: Dr. Robert Eichenberger (1 copy)

Commandant, U.S. Army, Air Defense School, Ft. Bliss, TX 79916 - Attn: Air Defense Agency (1 copy)
ATSA-CTD-MS (1 copy)

Commanding General, U.S. Army Combat Dev. Command, Ft. Belvoir, VA 22060 - Attn: Director of Material, Missile Div. (1 copy)

Commander, U.S. Army Training & Doctrine Command, Ft. Monroe, VA 23651 - Attn: ATCD-CF (1 copy)

Commander, U.S. Army Frankford Arsenal, Philadelphia, PA 19137 - Attn: Mr. M. Elnick SARFA-FCD Bldg. 201-3 (1 copy)

Commander, U.S. Army Electronics Command, Ft. Monmouth, NJ 07703 - Attn: AMSEL-CT-L, Dr. R.G. Buser (1 copy)

Commander, U.S. Army Combined Arms Combat Developments Activity, Ft. Leavenworth, KS 66027 (1 copy)

National Security Agency, Ft. Geo. G. Meade, MD 20755 - Attn: R.C. Foss A763 (1 copy)

Deputy Commandant for Combat & Training Developments, U.S. Army Ordnance Center and School, Aberdeen Proving Ground, MD 21005
Attn: ATSL-CTD-MS-R (1 copy)

Commanding Officer, USACDC CBR Agency, Ft. McClellan, AL 36201 - Attn: CDCCBR-MR (Mr. F.D. Poer) (1 copy)

DISTRIBUTION LIST (Continued)

Department of the Navy, Office of the Chief of Naval Operations, The Pentagon 5C739, Washington, D.C. 20350 - Attn: (OP 982F3) (1 copy)

Office of Naval Research Branch Office, 495 Summer Street, Boston, MA 02210 - Attn: Dr. Fred Quelle (1 copy)

Department of the Navy, Deputy Chief of Navy Material (Dev.), Washington, D.C. 20360 - Attn: Mr. R. Gaylord (MAT 032B) (1 copy)

Naval Missile Center, Point Mugu, CA 93042 - Attn: Gary Gibbs (Code 5352) (1 copy)

Naval Research Laboratory, Washington, D.C. 20375 - Attn: (Code 5503-EOTPO) (1 copy)
Dr. P. Livingston - Code 5560 (1 copy)
Dr. A. I. Schindler - Code 6000 (1 copy)
Dr. H. Shenker - Code 5504 (1 copy)
Mr. D.J. McLaughlin - Code 5560 (1 copy)
Dr. John L. Walsh - Code 5503 (1 copy)

High Energy Laser Project Office, Department of the Navy, Naval Sea Systems Command, Washington, D.C. 20360 - Attn: Capt. A. Skolnick, USN (PM 22) (1 copy)

Superintendent, Naval Postgraduate School, Monterey, CA 93940 - Attn: Library (Code 2124) (1 copy)

Navy Radiation Technology, Air Force Weapons Lab (NLO), Kirtland AFB, NM 87117 (1 copy)

Naval Surface Weapons Center, White Oak, Silver Spring, MD 20910 - Attn: Dr. Leon H. Schindel (Code 310) (1 copy)
Dr. E. Leroy Harris (Code 313) (1 copy)
Mr. K. Enkenhaus (Code 034) (1 copy)
Mr. J. Wise (Code 047) (1 copy)
Technical Library (1 copy)

U.S. Naval Weapons Center, China Lake, CA 93555 - Attn: Technical Library (1 copy)

HQ USAF (AF/RDPS), The Pentagon, Washington, D.C. 20330 - Attn: Lt. Col. A.J. Chiota (1 copy)

HQ AFSC/XRLW, Andrews AFB, Washington, D.C. 20331 - Attn: Maj. J.M. Walton (1 copy)

HQ AFSC (DLCAW), Andrews AFB, Washington, D.C. 20331 - Attn: Maj. H. Axelrod (1 copy)

Air Force Weapons Laboratory, Kirtland AFB, NM 87117 - Attn: LR (1 copy)
AL (1 copy)

HQ SAMSO (XRTD), P.O. Box 92960, Worldway Postal Center, Los Angeles, CA 90009 - Attn: Lt. Dorian DeMaio (XRTD) (1 copy)

AF Avionics Lab (TEO), Wright Patterson AFB, OH 45433 - Attn: Mr. K. Hutchinson (1 copy)

Dept. of the Air Force, Air Force Materials Lab. (AFSC), Wright Patterson AFB, OH 45433 - Attn: Maj. Paul Elder (LPS) (1 copy)
Laser Window Group

HQ Aeronautical Systems Div., Wright Patterson AFB, OH 45433 - Attn: XRF - Mr. Clifford Fawcett (1 copy)

Rome Air Development Command, Griffiss AFB, Rome, NY 13440 - Attn: Mr. R. Urtz (OCSE) (1 copy)

HQ Electronics Systems Div. (ESL), L.G. Hanscom Field, Bedford, MA 01730 - Attn: Mr. Alfred E. Anderson (XRT) (1 copy)
Technical Library (1 copy)

Air Force Rocket Propulsion Lab., Edwards AFB, CA 93523 - Attn: B.R. Bornhorst, (LKCG) (1 copy)

Air Force Aero Propulsion Lab., Wright Patterson AFB, OH 45433 - Attn: Col. Walter Moe (CC) (1 copy)

Dept. of the Air Force, Foreign Technology Division, Wright Patterson AFB, OH 45433 - Attn: PDTN (1 copy)

Commandant of the Marine Corps, Scientific Advisor (Code RD-1), Washington, D.C. 20380 (1 copy)

Aerospace Research Labs., (AP), Wright Patterson AFB, OH 45433 - Attn: Lt. Col. Max Duggins (1 copy)

Defense Intelligence Agency, Washington, D.C. 20301 - Attn: Mr. Seymour Berler (DTIB) (1 copy)

Central Intelligence Agency, Washington, D.C. 20505 - Attn: Mr. Julian C. Nall (1 copy)

Analytic Services, Inc., 5613 Leesburg Pike, Falls Church, VA 22041 - Attn: Dr. John Davis (1 copy)

Aerospace Corp., P.O. Box 92957, Los Angeles, CA 90009 - Attn: Dr. G.P. Millburn (1 copy)

Airesearch Manuf. Co., 9851-9951 Sepulveda Blvd., Los Angeles, CA 90009 - Attn: Mr. A. Colin Stancliffe (1 copy)

Atlantic Research Corp., Shirley Highway at Edsall Road, Alexandria, VA 22314 - Attn: Mr. Robert Naismith (1 copy)

Avco Everett Research Lab., 2385 Revere Beach Parkway, Everett, MA 02149 - Attn: Dr. George Sutton (1 copy)
Dr. Jack Daugherty (1 copy)

Battelle Columbus Laboratories, 505 King Avenue, Columbus, OH 43201 - Attn: Mr. Fred Tietzel (STPIAC) (1 copy)

Bell Aerospace Co., Buffalo, NY 14240 - Attn: Dr. Wayne C. Solomon (1 copy)

Boeing Company, P.O. Box 3999, Seattle, WA 98124 - Attn: Mr. M.I. Gamble (2-, 460, MS 8C-88) (1 copy)

Electro-Optical Systems, 300 N. Halstead, Pasadena, CA 91107 - Attn: Dr. Andrew Jensen (1 copy)

ESL, Inc., 495 Java Drive, Sunnyvale, CA 94086 - Attn: Arthur Einhorn (1 copy)

DISTRIBUTION LIST (Continued)

General Electric Co., Space Division, P.O. Box 8555, Philadelphia, PA 19101 - Attn: Dr. R.R. Sigismonti (1 copy)

General Electric Co., 100 Plastics Avenue, Pittsfield, MA 01201 - Attn: Mr. D.G. Harrington (Rm. 1044) (1 copy)

General Research Corp., P.O. Box 3587, Santa Barbara, CA 93105 - Attn: Dr. R. Holbrook (1 copy)

General Research Corp., 1501 Wilson Blvd., Suite 700, Arlington, VA 22209 - Attn: Dr. Giles F. Crimi (1 copy)

Hercules, Inc., Industrial System Dept., Wilmington, DE 19899 - Attn: Dr. R.S. Voris (1 copy)

Herculer, Inc., P.O. Box 210, Cumberland, MD 21502 - Attn: Dr. Ralph R. Preckel (1 copy)

Hughes Research Labs., 3011 Malibu Canyon Road, Malibu, CA 90265 - Attn: Dr. D. Forster (1 copy)

Hughes Aircraft Co., Aerospace Group - Systems Division, Canoga Park, CA 91304 - Attn: Dr. Jack A. Alcalay (1 copy)

Hughes Aircraft Co., Centinela and Teale Streets, Bldg. 6, MS E-125, Culver City, CA 90230 - Attn: Dr. William Yates (1 copy)

Institute for Defense Analyses, 400 Army-Navy Drive, Arlington, VA 22202 - Attn: Dr. Alvin Schnitzler (1 copy)

Johns Hopkins University, Applied Physics Lab., 8621 Georgia Avenue, Silver Spring, MD 20910 - Attn: Dr. Albert M. Stone (1 copy)

Lawrence Livermore Laboratory, P.O. Box 808, Livermore, CA 94550 - Attn: Dr. R.E. Kidder (1 copy)
Dr. E. Teller (1 copy)
Dr. Joe Fleck (1 copy)

Los Alamos Scientific Laboratory, P.O. Box 1663, Los Alamos, NM 87544 - Attn: Dr. Keith Boyer (1 copy)

Lulejian and Associates, Inc., Del Amo Financial Center, 21515 Hawthorne Blvd. - Suite 500, Torrance, CA 90503 (1 copy)

Lockheed Palo Alto Res. Lab., 3251 Hanover St., Palo Alto, CA 94303 - Attn: L.R. Lunsford, Orgn. 52-24, Bldg. 201 (1 copy)

Mathematical Sciences Northwest, Inc., P.O. Box 1887, Bellevue, WN 98009 - Attn: Dr. Abraham Hertzberg (1 copy)

Martin Marietta Corp., P.O. Box 179, Mail Station 0471, Denver, CO 80201 - Attn: Mr. Stewart Chapin (1 copy)

Massachusetts Institute of Technology, Lincoln Laboratory, P.O. Box 73, Lexington, MA 02173 - Attn: Dr. S. Edelberg (1 copy)
Dr. L.C. Marquet (1 copy)

McDonnell Douglas Astronautics Co., 5301 Bolsa Avenue, Huntington Beach, CA 92647 - Attn: Mr. P.L. Klevatt, Dept. A3-830-BBFO, M/S 9 (1 copy)

McDonnell Douglas Research Labs., Dept. 220, Box 516, St. Louis, MO 63166 - Attn: Dr. D.P. Ames (1 copy)

MITRE Corp., P.O. Box 208, Bedford, MA 01730 - Attn: Mr. A.C. Cron (1 copy)

North American Rockwell Corp., Autonetics Div., Anaheim, CA 92803 - Attn: Mr. T.T. Kumagi, C/476 Mail Code HA18 (1 copy)

Northrop Corp., 3401 West Broadway, Hawthorne, CA 90250 - Attn: Dr. Gerard Hasserjian, Laser Systems Dept. (1 copy)

Dr. Anthony N. Pirri, Physical Sciences, Inc., 18 Lakeside Office Park, Wakefield, MA 01880 (1 copy)

RAND Corp., 1700 Main Street, Santa Monica, CA 90406 - Attn: Dr. C.R. Culp/Mr. G.A. Carter (1 copy)

Raytheon Co., 28 Seyon Street, Waltham, MA 02154 - Attn: Dr. F.A. Horrigan (Res. Div.) (1 copy)

Raytheon Co., Boston Post Road, Sudbury, MA 01776 - Attn: Dr. C. Sonnenschien (Equip. Div.) (1 copy)

Raytheon Co., Bedford Labs, Missile Systems Div., Bedford, MA 01730 - Attn: Dr. H.A. Mehlhorn (1 copy)

Riverside Research Institute, 80 West End Street, New York, NY 10023 - Attn: Dr. L.H. O'Neill (1 copy)
Dr. John Bose (1 copy)
(HPEGL Library) (1 copy)

R&D Associates, Inc., P.O. Box 3580, Santa Monica, CA 90431 - Attn: Dr. R.E. LeLevier (1 copy)

Rockwell International Corporation, Rocketdyne Division, Albuquerque District Office, 3636 Menaul Blvd., NE, Suite 211, Albuquerque, NM 87110 - Attn: C.K. Kraus, Mgr. (1 copy)

SANDIA Corp., P.O. Box 5800, Albuquerque, NM 87115 - Attn: Dr. Al Narath (1 copy)

Stanford Research Institute, Menlo Park, CA 94025 - Attn: Dr. F.T. Smith (1 copy)

Science Applications, Inc., 1911 N. Ft. Meyer Drive, Arlington, VA 22209 - Attn: L. Peckam (1 copy)

Science Applications, Inc., P.O. Box 328, Ann Arbor, MI 48103 - Attn: R.E. Meredith (1 copy)

Science Applications, Inc., 6 Preston Court, Bedford, MA 01703 - Attn: R. Greenberg (1 copy)

Science Applications, Inc., P.O. Box 2351, La Jolla, CA 92037 - Attn: Dr. John Asmus (1 copy)

Systems, Science and Software, P.O. Box 1620, La Jolla, CA 92037 - Attn: Alan F. Klein (1 copy)

Systems Consultants, Inc., 1050 31st Street, NW, Washington, D.C. 20007 - Attn: Dr. R.B. Keller (1 copy)

Thiokol Chemical Corp., WASATCH Division, P.O. Box 524, Brigham City, UT 84302 - Attn: Mr. J.E. Hansen (1 copy)

TRW Systems Group, One Space Park, Bldg. R-1, Rm. 1050, Redondo Beach, CA 90278 - Attn: Mr. Norman Campbell (1 copy)

United Technologies Research Center, 400 Main Street, East Hartford, CT 06108 - Attn: Mr. G.H. McLafferty (3 copies)

DISTRIBUTION LIST (Continued)

United Technologies Research Center, Pratt and Whitney Aircraft Div., Florida R&D Center, West Palm Beach, FL 33402 Attn: Dr. R. A. Schmidtke (1 copy)
Mr. Ed Pinsley (1 copy)

VARIAN Associates, EIMAC Division, 301 Industrial Way, San Carlos, CA 94070 - Attn: Mr. Jack Quinn (1 copy)

Vought Systems Division, LTV Aerospace Corp., P.O. Box 5907, Dallas, TX 75222 - Attn: Mr. F. G. Simpson, MS 254142 (1 copy)

Westinghouse Electric Corp., Defense and Space Center, Balt-Wash. International Airport - Box 746, Baltimore, MD 21203 - Attn: Mr. W. F. List (1 copy)

Westinghouse Research Labs., Beulah Road, Churchill Boro, Pittsburgh, PA 15235 - Attn: Dr. E. P. Riedel (1 copy)

United Technologies Research Center, East Hartford, CT 06108 - Attn: A. J. DeMaria (1 copy)

Airborne Instruments Laboratory, Walt Whitorian Road, Melville, NY 11746 - Attn: F. Pace (1 copy)

General Electric R&D Center, Schenectady, NY 12305 - Attn: Dr. Donald White (1 copy)

Cleveland State University, Cleveland, OH 44115 - Attn: Dean Jack Soules (1 copy)

EXXON Research and Engineering Co., P.O. Box 8, Linden, NJ 07036 - Attn: D. Grafstein (1 copy)

University of Maryland, Department of Physics and Astronomy, College Park, MD 20742 - Attn: D. Currie (1 copy)

Sylvania Electric Products, Inc., 100 Fergeson Drive, Mountain View, CA 94040 - Attn: L. M. Osterink (1 copy)

North American Rockwell Corp., Autonetics Division, 3370 Miraloma Avenue, Anaheim, CA 92803 - Attn: R. Gudmundsen (1 copy)

Massachusetts Institute of Technology, 77 Massachusetts Avenue, Cambridge, MA 02138 - Attn: Prof. A. Javan (1 copy)

Lockheed Missile & Space Co., Palo Alto Research Laboratories, Palo Alto, CA 94304 - Attn: Dr. R. C. Ohlman (1 copy)

ILC Laboratories, Inc., 164 Commercial Street, Sunnyvale, GA 94086 - Attn: L. Noble (1 copy)

University of Texas at Dallas, P.O. Box 30365, Dallas, TX 75230 - Attn: Prof. Carl B. Collins (1 copy)

Polytechnic Institute of New York, Rt. 110, Farmingdale, NY 11735 - Attn: Dr. William T. Walter (1 copy)